TECH LIBRARY KAFB, NM
0060199

NASA CONTRACTOR REPORT

NASA CR-666

NASA CR-6
C.1

LOAN COPY: RETURN TO
AFWL (WLIL-2)
KIRTLAND AFB, N MEX

DYNAMIC CHARACTERISTICS OF SQUARE PLATES BY PASSIVE ANALOG SIMULATION

by R. L. Barnoski

Prepared by
MEASUREMENT ANALYSIS CORPORATION
Los Angeles, Calif.
for George C. Marshall Space Flight Center

NATIONAL AERONAUTICS AND SPACE ADMINISTRATION • WASHINGTON, D. C. • JANUARY 1967

TECH LIBRARY KAFB, NM

0060199

NASA CR-666

DYNAMIC CHARACTERISTICS OF SQUARE PLATES BY PASSIVE ANALOG SIMULATION

By R. L. Barnoski

Distribution of this report is provided in the interest of information exchange. Responsibility for the contents resides in the author or organization that prepared it.

Prepared under Contract No. NAS 8-20020 by
MEASUREMENT ANALYSIS CORPORATION
Los Angeles, Calif.

for George C. Marshall Space Flight Center

NATIONAL AERONAUTICS AND SPACE ADMINISTRATION

For sale by the Clearinghouse for Federal Scientific and Technical Information
Springfield, Virginia 22151 – Price $2.50

TABLE OF CONTENTS

	Page
Introduction	v
1. Circuit Derivation for the Lateral Vibration of Rectangular Plates	1
1.1 General Background	1
1.2 Strain Energy Procedure	4
2. Analog Computer Study	14
2.1 Scope of the Program	14
2.2 Physical Structures	15
2.3 Scale Factors and Setting Values	19
2.4 Computer Circuits	22
3. Computer Results	31
3.1 Flexible Boundary Studies	31
3.2 Damper Effects Study	36
3.3 Errors	42
References	48

INTRODUCTION

This report considers the derivation and illustrates the use of a passive analog circuit to investigate dynamic properties of square plates. Two basic studies are conducted:

1. Effect of boundary bending flexibility on the fundamental modal frequency for both uniform and tapered geometry.
2. Effect of edge dampers and a uniformly distributed loading on the frequency response characteristics of a uniform square plate.

The results of these two studies are displayed as plots and charts based upon data obtained from the passive analog computer.

The analog circuit employs mobility concepts and is derived essentially by equating the strain energy and kinetic energy associated with the lateral vibration of an arbitrary rectangular plate to the energy of the analog circuit. The resultant analog circuit can be applied to any rectangular plates with nonuniform physical properties, with arbitrary boundary conditions, and with any arbitrary deterministic and/or random loading.

1. CIRCUIT DERIVATION FOR THE LATERAL VIBRATION OF RECTANGULAR PLATES

1.1 GENERAL BACKGROUND

The use of electrical analogies to solve physical problems is not a new concept. As early as 1845, Kirchhoff (Reference 7) used analog circuits to study current flow characteristics through a circular disk. Two of the earlier works dealing with analysis of structures by electrical analogs date to Firestone (Reference 4) in 1933 and Bush (Reference 3) in 1934. To gain a more complete historical perspective of electro-analogic methods, in general, the reader is directed to the work of Higgins (Reference 6).

Attention is focused in this discussion on the derivation and use of a passive electrical analog for the lateral vibration characteristics of a flat, rectangular plate. As contrasted with active electrical analogs consisting of operational amplifier circuits, a passive analog is a circuit consisting of some combination of passive circuit components, i. e., resistors, inductors, capacitors, and transformers. A direct or one-to-one correspondence exists between components in the electrical network and the elements of the mechanical system. In many instances, a topological similarity also exists between the mechanical system and electrical circuit so that an intuitive understanding of the electrical model is promoted.

Classically speaking, the passive circuit used here for dynamics analyses is a <u>mobility analog or force-current, velocity-voltage electrical network</u>. This circuit is the <u>dual</u> of the mechanical impedance analog which may be classically defined as a force-voltage, velocity-current electrical network. Consistent with the mobility definition, flexibility is proportional to inductance, mass to capacitance, and viscous damping to resistance. All

nodal voltages are equivalent to velocities at specific locations on the mechanical structure and all currents are equivalent to forces or moments. The electrical impedances in the passive network are equivalent to mechanical mobilities and the electrical admittances are equivalent to mechanical impedances. In Chapter 10 of Reference 5, Freberg provides an introduction to mobility concepts with application to linear mechanical oscillators.

Although the derivation procedures discussed by MacNeal (Reference 8) and Barnoski (Reference 1) are applicable, a strain energy approach is used to derive a passive analog for the rectangular plate. Such an approach is consistent with the work of Ryder (Reference 9) and is shown schematically as Figure 1. This same strain-energy procedure is used by Barnoski and Freberg to develop analog circuits for the elasticity equations in three dimensions (Reference 2).

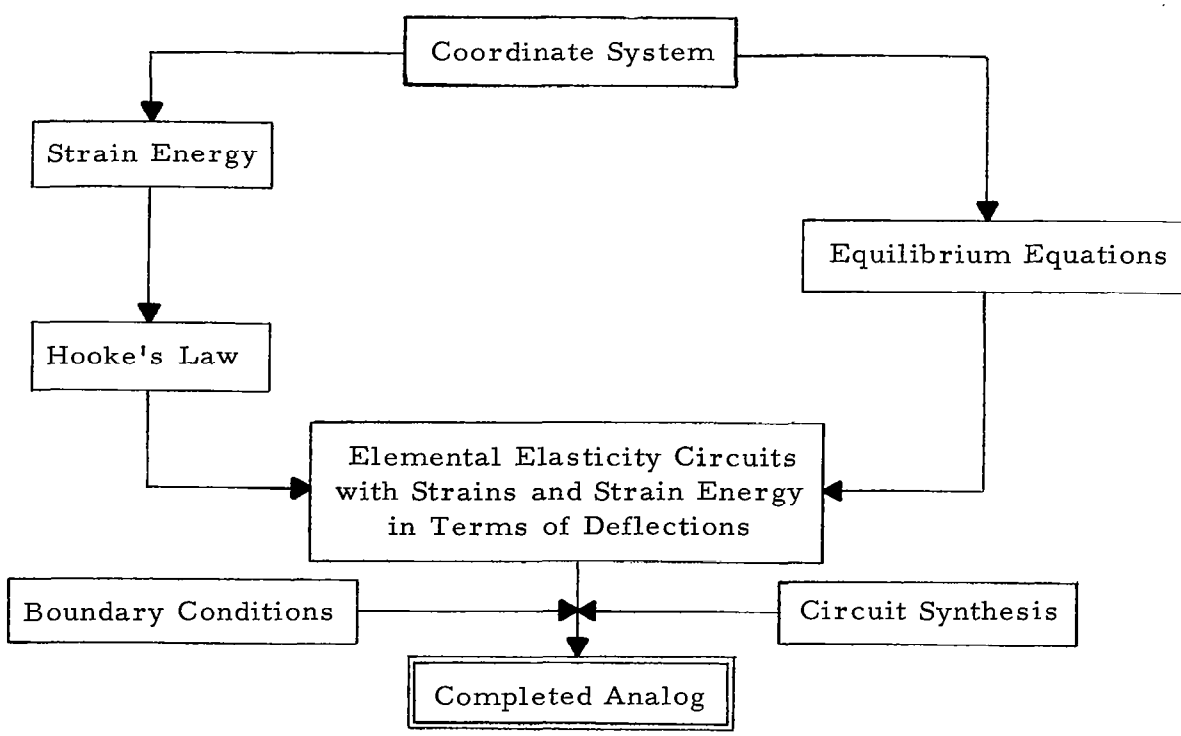

Figure 1. Strain Energy-Compatibility Approach for a Passive Electrical Analog of an Elastic Structural System

Elastic strain energy for a specific structure is first expressed in finite-difference form and then equated to twice the electrical power. Kirchhoff's and Ohm's laws are imposed to yield an analog circuit. This circuit is a force-current, displacement-voltage analog and, to retain the mobility orientation, is appropriately called a static-mobility analog. Such an analog describes the static behavior of a difference segment of structure and can be routinely converted to a dynamic analog by

- defining all nodal voltages to be mechanically equivalent to velocities
- changing all resistors to inductors
- adding capacitors to ground at the deflection nodes
- adding resistors if viscous damping is to be included.

For use on a passive element computer, the circuit for a difference segment of a rectangular plate is interconnected to form a complete electrical model for the lateral vibration of a rectangular plate.

For mechanical systems described mathematically as second-order, ordinary differential equations in time, such as a system of interconnected mechanical oscillators, the mobility analog is a Resistor-Inductor-Capacitor (RLC) network. For undamped distributed mechanical systems described mathematically as higher-order, partial differential equations in space and time, the mobility analog is a LC-Transformer (LCT) network. This network approximates the original distributed system as a finite-difference mathematical model and is mechanically equivalent to a lumped-parameter model. The transformer interconnections account for the spatial geometry defined by the spatial derivatives in the original differential equation and represent one of the more difficult tasks in analog derivation. If viscous damping is included, resistors then appear in the LCT analog. The work of MacNeal (Reference 8) discusses in detail derivation concepts for simpler distributed elastic structures and is one of the more complete writings dealing with passive analogs and passive analog computers.

1.2 STRAIN ENERGY PROCEDURE

The physical system is depicted in Figure 2 as a differential plate segment of dimensions dx, dy and of thickness h. The forces correspond to shear (Q_x and Q_y) per unit length, bending moments per unit length (M_{xx} and M_{yy}), and twisting moments (M_{xy} and M_{yx}) per unit length. Deflections are assumed to be small in comparison to the plate thickness and strain in the middle plane of the plate is assumed negligible.

The strain energy per unit **area** of a rectangular, differential plate element in bending is given as Reference 10, page 46),

$$2V_0 = D\left\{\left(\frac{\partial^2 w}{\partial x^2}\right)^2 + \left(\frac{\partial^2 w}{\partial y^2}\right)^2 + 2\nu\frac{\partial^2 w}{\partial x^2}\cdot\frac{\partial^2 w}{\partial y^2}\right\} + 2D(1-\nu)\left\{\frac{\partial^2 w}{\partial x\,\partial y}\right\}^2 \tag{1}$$

where the plate flexural rigidity is

$$D = \frac{Eh^3}{12(1-\nu^2)} \tag{2}$$

and E is Young's modulus, w is the lateral deflection of the plate from static equilibrium, x and y are the spatial coordinates in the x and y directions, and ν is Poisson's ratio. In slightly different form the strain energy expression may be rewritten as

$$2V_0 = D\left\{\frac{\partial^2 w}{\partial x^2} + \nu\frac{\partial^2 w}{\partial y^2}\right\}^2 + D(1-\nu^2)\left\{\frac{\partial^2 w}{\partial y^2}\right\}^2 + 2D(1-\nu)\left\{\frac{\partial^2 w}{\partial x\,\partial y}\right\}^2 \tag{3}$$

Differential Plate Segment

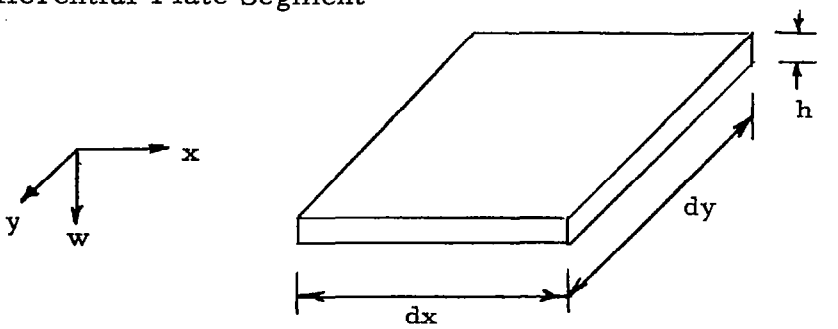

Bending and Twisting Moments

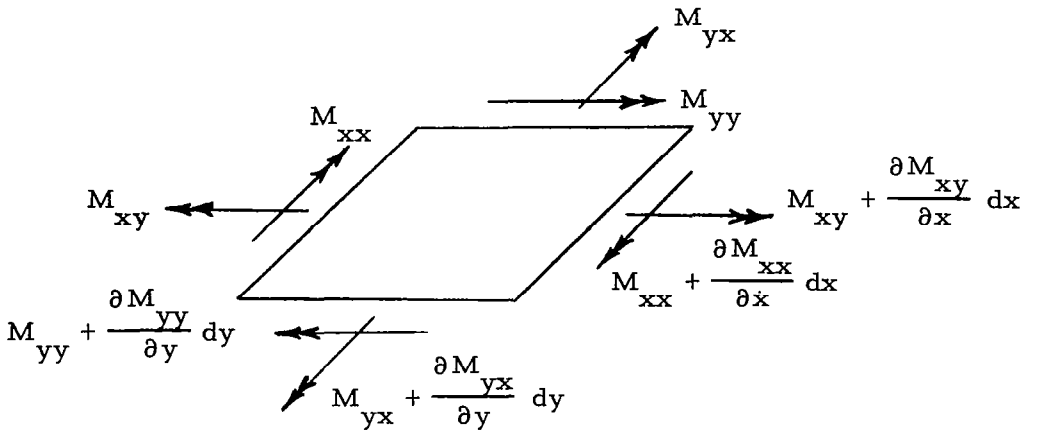

Shear Forces

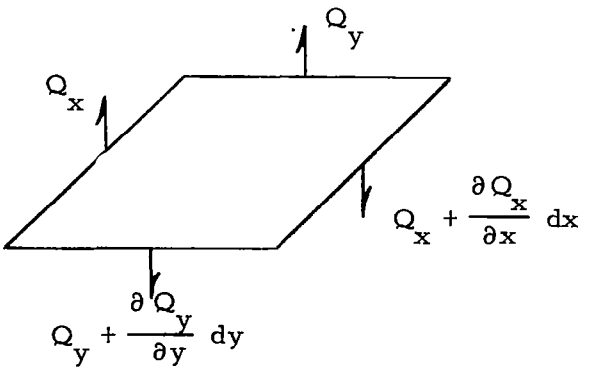

Figure 2. Differential Segment of a Rectangular Plate in Bending

The first two terms denote the strain energy due to bending and the last term specifies the strain energy due to twisting.

For a plate element of difference dimensions (Δx, Δy,), the strain energy may be expressed in finite difference form

$$2V = D\frac{\Delta y}{\Delta x}\left\{\Delta_x(\theta_x) + \nu\frac{\Delta x}{\Delta y}\Delta_y(\theta_y)\right\}^2 + D\frac{\Delta x}{\Delta y}(1-\nu^2)\left\{\Delta_y(\theta_y)\right\}^2 + 2D\frac{\Delta y}{\Delta x}(1-\nu)\left\{\Delta_x(\theta_y)\right\}^2 \tag{4}$$

where the directional slopes in bending are defined as

$$\theta_x = \frac{\partial w}{\partial x} \qquad \theta_y = \frac{\partial w}{\partial y} \tag{5}$$

Equating twice the strain energy with the power dissipation in a resistor yields

$$2V = P = \frac{e^2}{R} \tag{6}$$

where e is the positive voltage drop across the resistor R. Defining the bracketed terms of Eq. (4) as voltages, the strain energy expression reduces in form to Eq. (6) and can be simulated electrically by the power

dissipation of three resistors. Using a 3 x 3 finite-difference grid, an analog circuit electrically equivalent to the strain energy expression of Eq. (4) is displayed as Figures 2-a, 2-b and 2-c with the circuit elements given by Figure 2-d.

The finite difference grid shows nine rectangular plate segments where the x-difference positions are given by capital letters and the y-difference positions as numbers. Thus, the numerical difference between two consecutive letters is the difference length Δx whereas the difference between two consecutive digits is the difference length Δy. The positive signs indicate the transformer polarity and define the manner in which the transformers must be interconnected to form the proper spatial geometry.

Although sketched as three distinct circuits: (1) the lateral deflection circuit, (2) the θ_x slope circuit, and (3) the θ_y circuit, these circuits are magnetically coupled by the transformers. Transformers 2 and 3 couple the lateral deflection with the θ_x and θ_y slope circuits, respectively. Transformer 1 accounts for the Poisson coupling in the first bracketed term of Eq. (4) by constraining the θ_x and θ_y circuits. Resistors R_1 and R_2 account for the bending strain energy while the R_3 resistor accounts for the twisting strain energy. The resistor magnitudes are noted as reciprocals of the coefficients in Eq. (4).

Since the magnitude and direction of forces and moments are required in stress analyses, it is necessary to calculate the mechanical equivalents of the currents flowing through the various resistors. The relationships between the moments and curvature are defined by Timoshenko and Krieger (Section 21 of Reference 10) as Eq. (7).

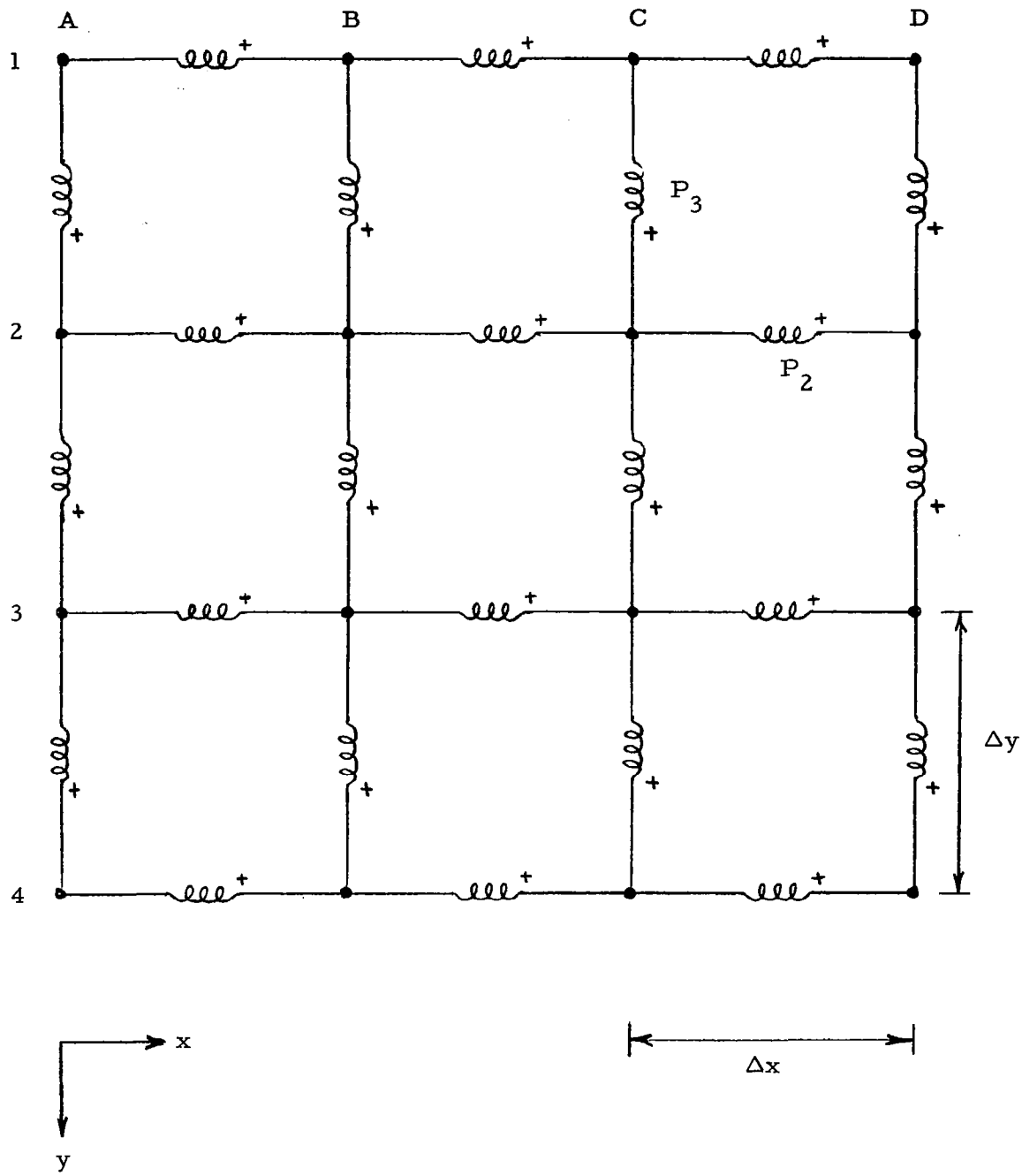

Figure 2-a. Deflection Circuit (w) for a Rectangular Plate in Bending Assuming Small Deflection Theory

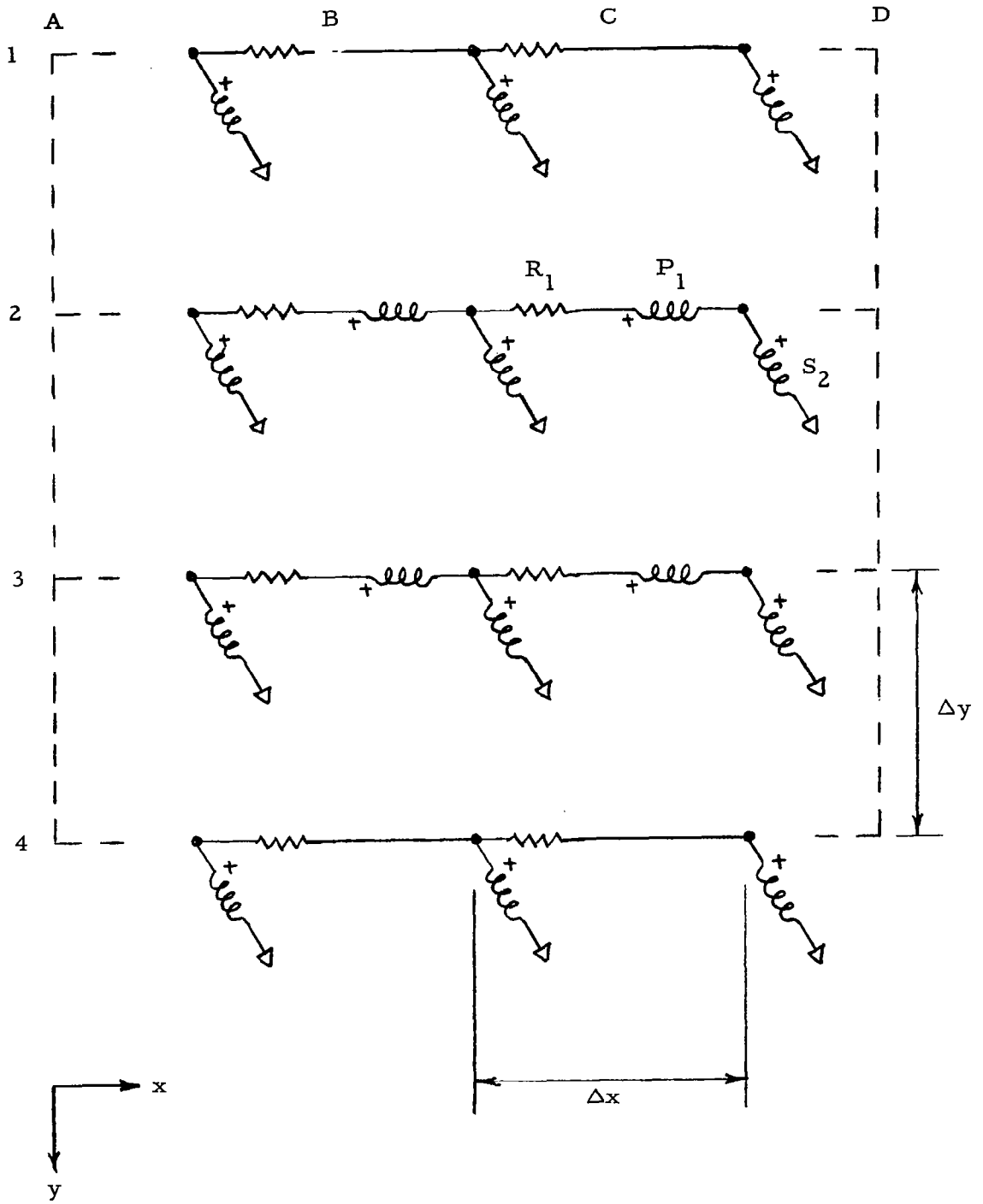

Figure 2-b. θ_x Circuit for a Rectangular Plate in Bending Assuming Small Deflection Theory

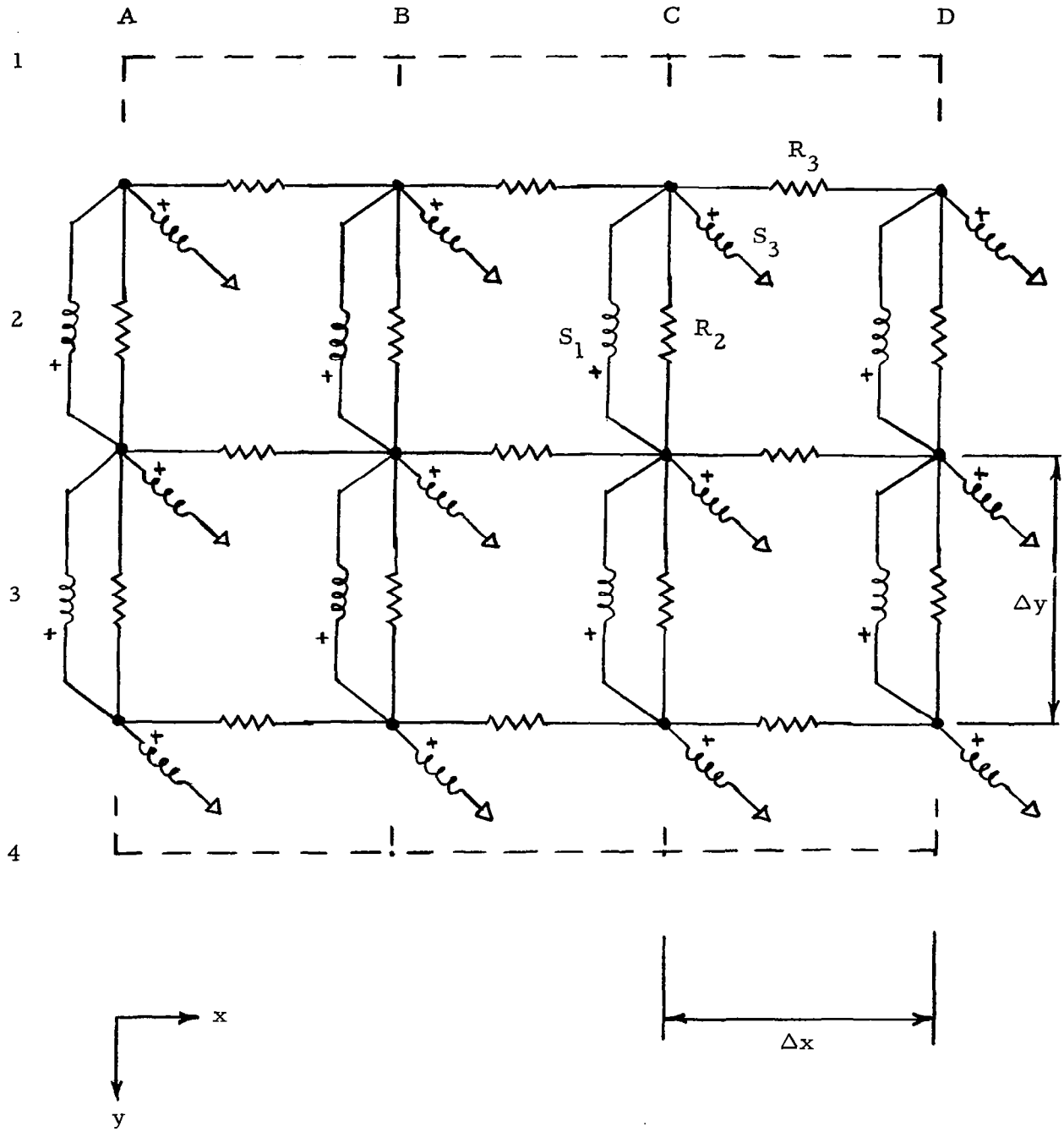

Figure 2-c. θ_y Circuit for a Rectangular Plate in Bending Assuming Small Deflection Theory

Circuit Elements	
Resistors	Transformers
$R_1 = \frac{\Delta x}{\Delta y} \cdot \frac{1}{D}$	$\frac{P_1}{S_1} = \nu \frac{\Delta x}{\Delta y}$
$R_2 = \frac{\Delta y}{\Delta x} \cdot \frac{1}{D(1 - \nu^2)}$	$\frac{P_2}{S_2} = \Delta x$
$R_3 = \frac{\Delta x}{\Delta y} \cdot \frac{1}{2D(1 - \nu)}$	$\frac{P_3}{S_3} = \Delta y$

$D = \frac{Eh^3}{12(1 - \nu^2)}$ = flexural rigidity of the plate

E = Young's modulus

h = thickness of the plate

ν = Poisson's ratio

Δx = incremental x distance of the plate grid

Δy = incremental y distance of the plate grid

Figure 2-d. Element Values of the Circuits for a Rectangular Plate in Bending

$$M_{xx} = -D\left\{\frac{\partial(\theta_x)}{\partial x} + \nu\frac{\partial(\theta_y)}{\partial y}\right\}$$

$$M_{yy} = -D\left\{\frac{\partial(\theta_y)}{\partial y} + \nu\frac{\partial(\theta_x)}{\partial x}\right\} \tag{7}$$

$$M_{xy} = -M_{yx} = D(1 - \nu)\frac{\partial(\theta_y)}{\partial x}$$

where the term $\partial^2 w/\partial x \partial y$ is arbitrarily expressed as a partial derivative of the slope θ_y. Multiplying the M_{xx} bending moment by Poisson's ratio ν and adding the resultant expression to M_{yy} yields

$$-\left(M_{yy} + \nu M_{xx}\right) = D(1 - \nu^2)\left\{\frac{\partial^2 w}{\partial y^2}\right\} \tag{8}$$

Multiplying Eq. (8) by the difference length Δx and expressing the partial derivative in finite-difference form produces

$$-\Delta x(M_{yy} - \nu M_{xx}) = \frac{\Delta x}{\Delta y} D(1 - \nu^2)\Delta_y(\theta_y) \tag{9}$$

Noting $\Delta_y(\theta_y)$ corresponds to the voltage drop given by the second term of Eq. (4), i.e., the voltage drop across the R_2 resistor, Ohm's law states

the positive current flow through the R_2 resistor is

$$I_{R_2} = -(M_{yy} - \nu M_{xx}) \Delta x \tag{10}$$

In a similar manner, positive current flows through the R_1 and R_3 resistors are shown to be

$$\begin{aligned} I_{R_1} &= -M_{xx} \Delta y \\ I_{R_3} &= (M_{xy} - M_{yx}) \Delta y \end{aligned} \tag{11}$$

2. ANALOG COMPUTER STUDY

2.1 SCOPE OF PROGRAM

The intent is to examine the dynamic characteristics of a homogeneous square plate with uniform and nonuniform physical properties, with edge boundaries of varying bending flexibility, and with a distributed deterministic loading. The dynamic characteristics refer to the modal frequencies, mode shapes and the magnitude of velocity to force frequency response functions. Two basic studies are conducted:

1. Effect of Boundary Bending Flexibility on the Dynamic Characteristics for both Uniform and Tapered Geometry
2. Effect of Edge Dampers and a Uniform Distributed Loading on the Frequency Response Characteristics

The first study is designed to show the effect of a flexible boundary in bending on the fundamental mode shape, the associated modal frequency, and the maximum magnitude of velocity to force frequency response functions. The response function is measured near the geometric center of the plate. Two symmetric loading conditions are considered (1) partially distributed or limited area loading applied at the center of the plate, (2) a loading of constant magnitude uniformly distributed over the surface of the plate. All boundary conditions are varied uniformly from simply supported at all edges to fully clamped at all edges with intermediate values of bending flexibility.

For the tapered or nonuniform plates, the effect of a flexible boundary in bending on the fundamental mode shape and associated modal frequency is studied. The plates are tapered only in one direction with

thickness ratios at the boundaries of 1.33 and 2.00. These thickness ratios are called taper ratios in this discussion.

The second study is designed to show the effect of viscous dampers on the magnitude of the frequency response function for a square plate simply supported at all edges. The dampers are uniformly distributed around the edges of the plate and the dashpot settings are varied uniformly from simply supported boundaries to an arbitrary plausible value of viscous damping. The external loadings and location of the response function are the same as those in the first study.

2.2 PHYSICAL STRUCTURES

The basic structure is a flat, square aluminum plate with physical properties listed in Figure 3.

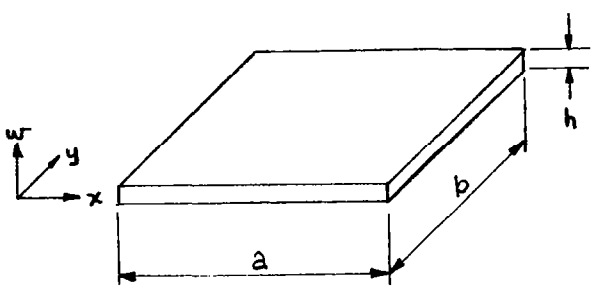

$$a = b = \ell = 12 \text{ in.}$$
$$h = 0.0625 \text{ in.}$$
$$E = 10.5 \times 10^6 \text{ lb/in.}^2$$
$$\rho = 0.10 \text{ lb/in.}^3$$
$$\nu = 0.3$$

Figure 3. Physical Properties of Square Plate

The positive directions are shown by the x, y and w coordinate system where w is the deflection from the static equilibrium position. Other notation shows a and b as the plate dimensions in the x and y directions (both equal to the length ℓ), h is the plate thickness, E is Young's modulus, ρ is the density of the material, and ν is Poisson's ratio.

The tapered plates vary in thickness with a constant slope in the x dimension as sketched in Figure 4.

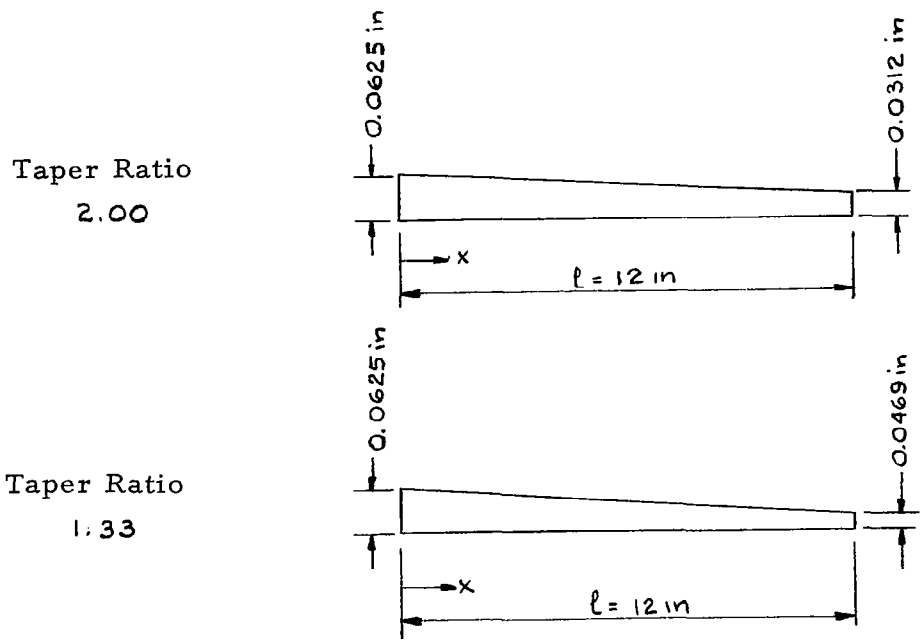

Figure 4. Cross-section of Tapered Plates

The taper ratio is defined as the ratio of the thickness at x = 0 to the thickness at x = ℓ.

Assuming small deflections and linearized elasticity theory, the equation of motion for a uniform rectangular plate is

$$\nabla^4 w + \frac{m_o}{D}\frac{\partial^2 w}{\partial t^2} = 0 \tag{12}$$

where the spatial operator, the plate flexural rigidity, and the plate mass per unit area are

$$\nabla^2 = \frac{\partial^2}{\partial x^2} + \frac{\partial^2}{\partial y^2}$$

$$D = \frac{E h^3}{12(1 - \nu^2)} = 235 \text{ lb-in.} \tag{13}$$

$$m_o = 1.62 \times 10^{-5} \frac{\text{lb-sec}^2}{\text{in.}^3}$$

Expressed as a function of the deflection w, this equation is noted as a fourth order, partial differential equation with constant coefficients. The deflection is understood to be a function of the spatial coordinates x and y, and of time t.

The solution to Eq. (12) is of the form

$$w(x, y, t) = \sum_m \sum_n \phi_{mn}(x, y)\, q_{mn}(t) \tag{14}$$

where m and n denote the number of half sines in the x and y directions for the mn mode, $\phi_{mn}(x, y)$ is the mn mode shape of the plate, and $q_{mn}(t)$ is the generalized coordinate associated with the mn mode. This solution is consistent with the modal theory of distributed structures and corresponds classically to the separation-of-variables technique in solving partial differential equations.

For simply-supported boundary conditions of all edges, the mode shapes are

$$\phi_{mn}(x, y) = \sin \frac{m\pi x}{\ell} \sin \frac{n\pi x}{\ell} \tag{15}$$

with the associated modal frequencies

$$f_{mn} = \frac{\pi}{2} \sqrt{\frac{D}{m_o}} \left(\frac{m^2}{a^2} + \frac{n^2}{b^2} \right) \text{ cps} \tag{16}$$

For a square plate, the modal frequencies reduce to

$$f_{mn} = \frac{\pi}{2\ell^2}(m^2 + n^2)\sqrt{\frac{D}{m_o}} \text{ cps} \tag{17}$$

Substituting the plate numerical values from Figure 3 into Eq. (17) produces

$$f_{mn} = 41.5\,(m^2 + n^2) \text{ cps} \tag{18}$$

2.3 SCALE FACTOR AND SETTING VALUES

To electrically set up the physical problem on an analog computer, the physical and geometric properties of the structure must be compatible with the element setting values on the analog computer. This is achieved through the use of the scale factors shown in Figure 5. Such factors are constants which interrelate the physical quantities in the mechanical and electrical systems and are discussed in detail by MacNeal in Reference 8

Compatible with mobility concepts, the strain energy of Eq. (4) is expressed in terms of the velocity; and, upon substitution of appropriate scale factors, the inductor and transformer settings become

$$L_1 = \left(\frac{P_\theta}{a}\right)^2 \frac{1}{D}\left(\frac{\Delta x}{\Delta y}\right) \qquad \frac{P_1}{S_1} = \nu\frac{\Delta x}{\Delta y}$$

$$L_2 = \left(\frac{P_\theta}{a}\right)^2 \frac{1}{D(1-\nu^2)}\left(\frac{\Delta y}{\Delta x}\right) \qquad \frac{P_2}{S_2} = \frac{\Delta x}{P_\theta} \tag{19}$$

$$L_3 = \left(\frac{P_\theta}{a}\right)^2 \frac{1}{2D(1-\nu)}\left(\frac{\Delta x}{\Delta y}\right) \qquad \frac{P_3}{S_3} = \frac{\Delta y}{P_\theta}$$

Forces	
$F = \frac{k}{a} I$	F = mechanical force
$M_\theta = \frac{kP_\theta}{a} I_\theta$	M_θ = bending moment
$T_\phi = \frac{kP_\phi}{a} I_\phi$	T_θ = torque or twisting moment
	I = current corresponding to F
	I_θ = current corresponding to M_θ
	I_ϕ = current corresponding to T_ϕ
Coordinate Motion	
$\dot{w} = \frac{ka}{N} e_{\dot{w}}$	$\dot{w}$ = lateral or linear velocity
$\dot{\theta} = \frac{ka}{NP_\theta} e_{\dot{\theta}}$	$\dot{\theta}$ = slope velocity
$\dot{\phi} = \frac{ka}{NP_\phi} e_{\dot{\phi}}$	$\dot{\phi}$ = angular (twisting) velocity
	t_m = real or mechanical time
	$e_{\dot{w}}$ = voltage corresponding to $\dot{w}$
	$e_{\dot{\theta}}$ = voltage corresponding to $\dot{\theta}$
	$e_{\dot{\phi}}$ = voltage corresponding to $\dot{\phi}$
$t_m = Nt_e$	$k, a, P_\theta, P_\phi, N$ = scaling constants
	t_e = electrical time

Figure 5. General Scale Factor Relationships for Mobility Analogs

Compared with the quantities shown in Figure 2-d, the inductor setting values differ from the resistor expressions by the square of P_θ/a. The first transformer remains unchanged whereas the second and third transformers differ by the P_θ scale factor.

To account for the kinetic energy of the mass associated with the finite difference grid, capacitors are added to each of the nodes in the deflection circuit. The capacitor magnitude at any node is given by

$$C = \left(\frac{a}{N}\right)^2 m_o \Delta x \, \Delta y \tag{20}$$

where Δx and Δy are the difference dimensions for the nodal element. The inductor and transformer settings of Eq. (19) plus the capacitor values given above are the electrical components required to simulate the lateral vibration of a difference segment of rectangular plate.

As a computational aid in computing setting values (and is particularly useful for uniform structures), the $L_1 C$ product is formed from terms in Eqs. (19) and (20) as

$$L_1 C = \pi^2 \left(\frac{\Delta x}{\ell}\right)^4 \left[\frac{1}{f_{11}\,(\text{elec})}\right]^2 \frac{1}{\left(\frac{P}{S}\right)^2} \tag{21}$$

where the transformer ratio is

$$\frac{P}{S} = \frac{\Delta x}{P_\theta} \tag{22}$$

and the fundamental electrical frequency is related to the fundamental modal frequency of a simply supported plate as

$$f_{11}\,(\text{elec}) = N f_{11}\,(\text{mech}) \tag{23}$$

Equation (21) is used to create families of curves in f_{11} (elec) for the transformer ratio P/S versus the L_1C product.

2.4 COMPUTER CIRCUITS

Based upon the number of available transformers, inductors, and capacitors in the passive analog computer, a 5 x 5 finite difference grid was adopted for the simulation of a full plate. Cascading the circuits of Figure 2, the resultant network for a 5 x 5 grid simulation of the lateral vibration of a rectangular plate appears as Figures 6. The components values are provided by Eqs. (19) and (20). Compared to the basic static circuits of Figure 2, capacitors have been added to the deflection circuit and resistors have been converted to inductors in the slope circuits. Symbolically, the inductors in Figures 6 are shown as resistors to minimize confusion between inductor symbols and transformer windings. These circuits remain unchanged for the tapered plates although the component setting values will vary from the setting values for a uniform plate.

The hexagonal figures at the circuit boundaries denote spatial positions along the edges of the plate. These are the circuit locations at which boundary conditions are simulated. For simply supported or fully clamped boundary conditions at all edges, the hexagons denote simple single-throw switches to ground which are either open or closed as shown in Figures 7 and 8. For boundary conditions with bending flexibility, the hexagons in the

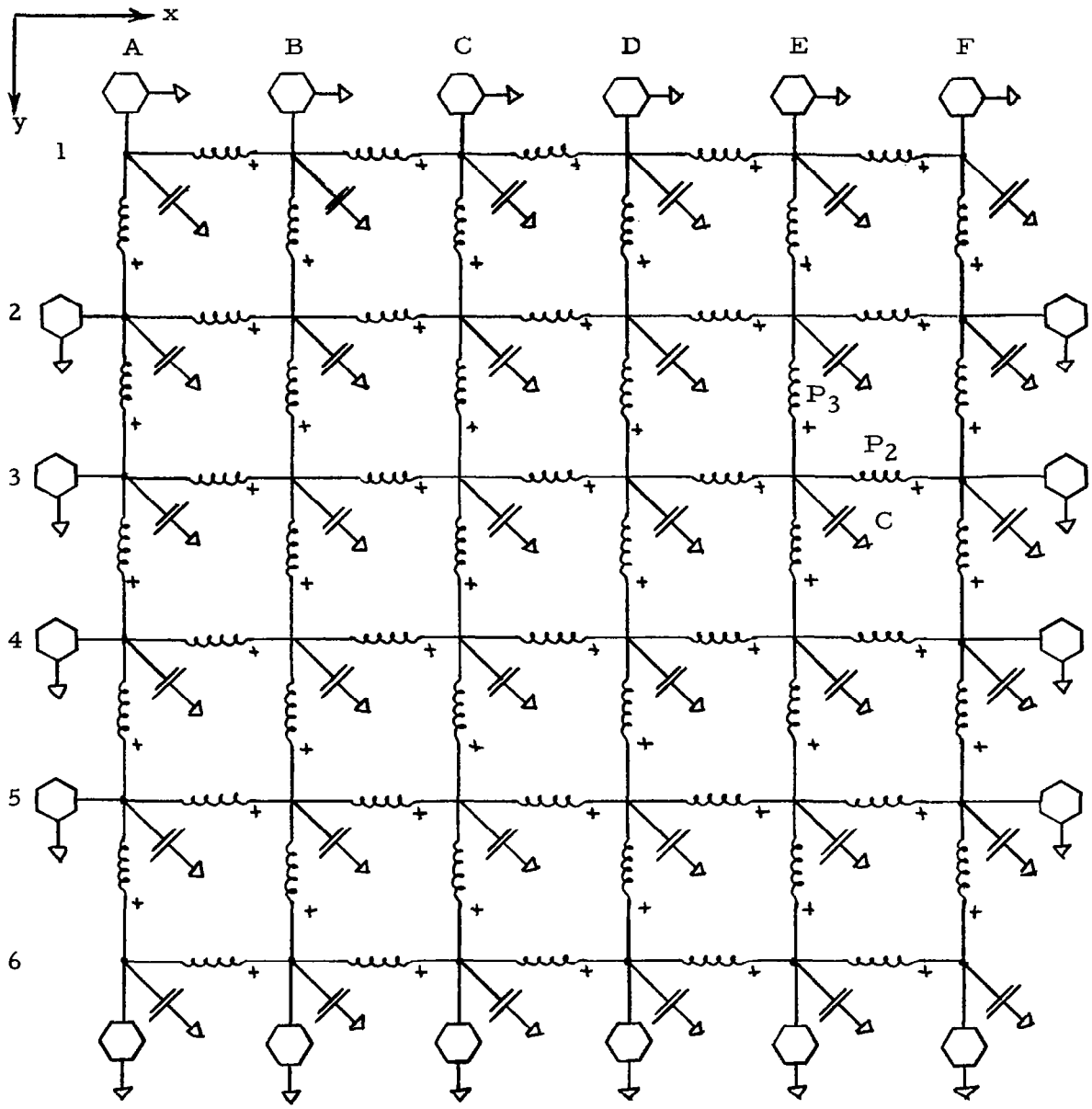

Figure 6-a. $\dot{w}$ Deflection Circuit for the Lateral Vibration of a Rectangular Plate

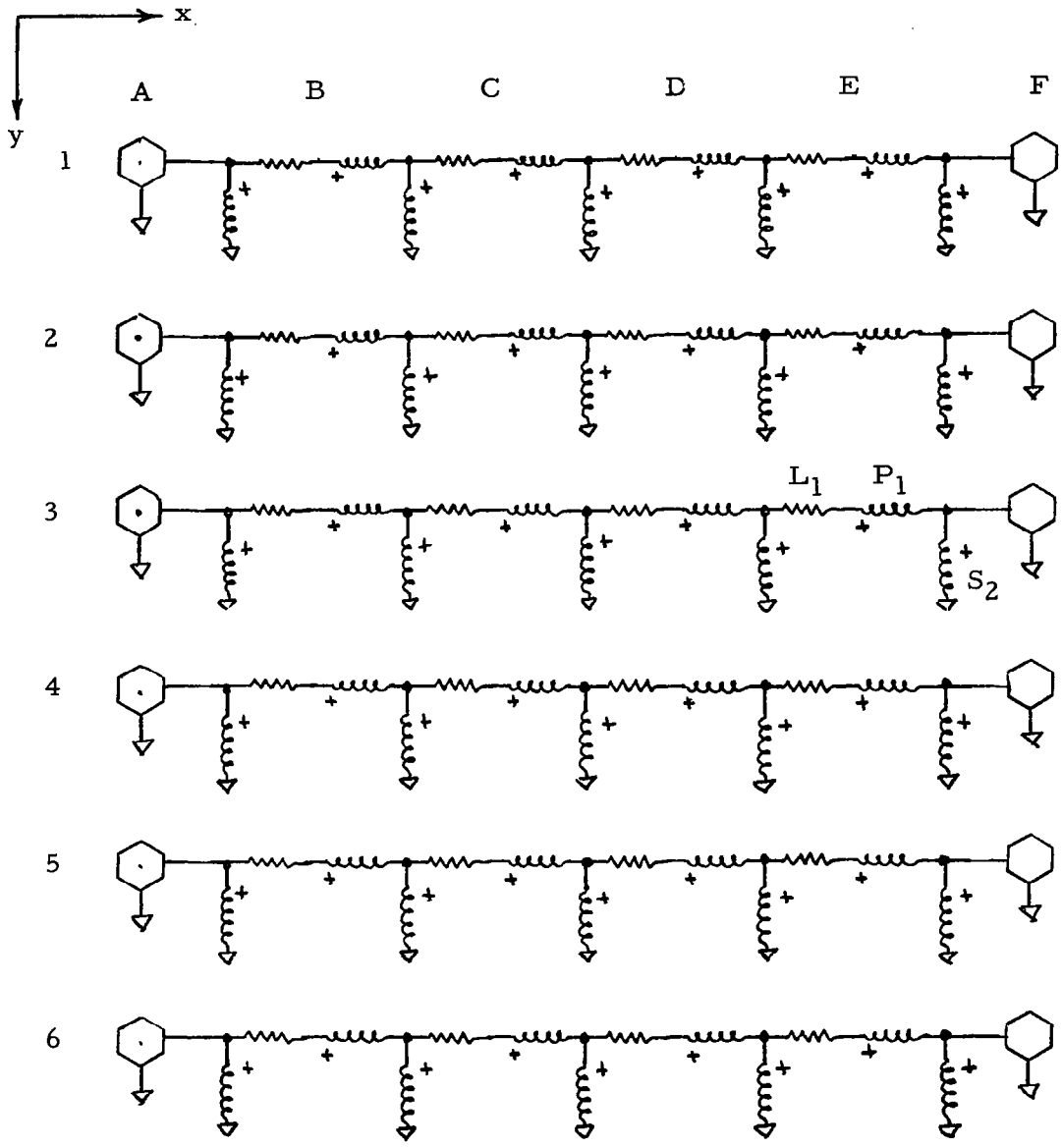

Figure 6-b. $\dot{\theta}_x$ Slope Circuit for the Lateral Vibration of a Rectangular Plate

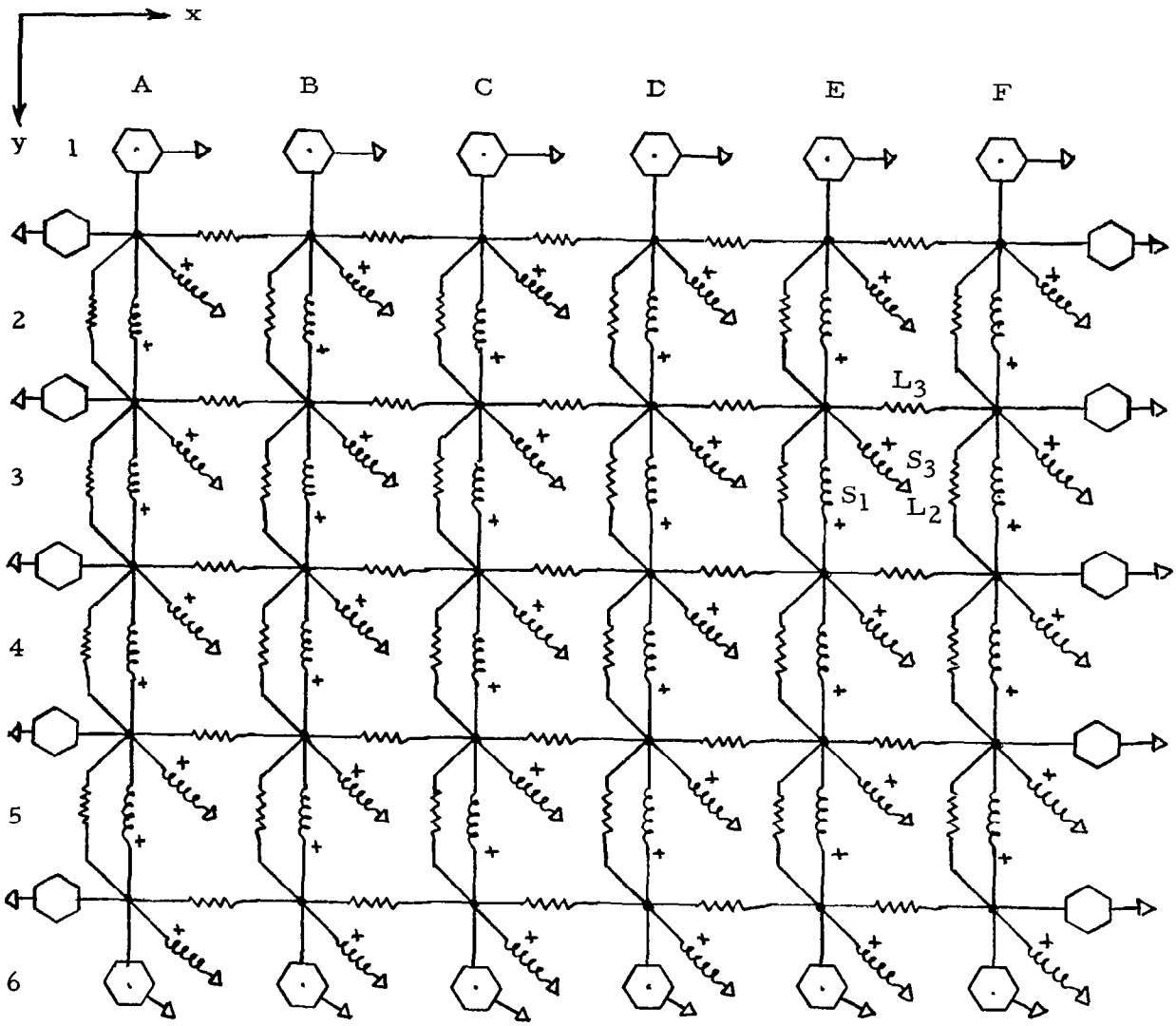

Figure 6-c. $\dot{\theta}_y$ Slope Circuit for the Lateral Vibration of a Rectangular Plate

	Analytical	Analog
Deflections	$w(x, 0) = 0$ $w(x, \ell) = 0$ $w(0, y) = 0$ $w(\ell, y) = 0$	$\dot{w}$ Circuit 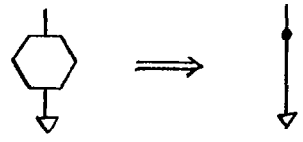
Moments	$M_{xx}(x, 0) = 0$ $M_{xx}(x, \ell) = 0$	$\dot{\theta}_x$ Circuit
	$M_{yy}(0, y) = 0$ $M_{yy}(\ell, y) = 0$	$\dot{\theta}_y$ Circuit 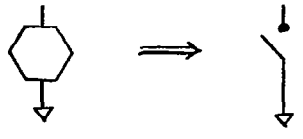
	$M_{xy}(0, y) = 0$ $M_{xy}(\ell, y) = 0$	$\dot{\theta}_y$ Circuit 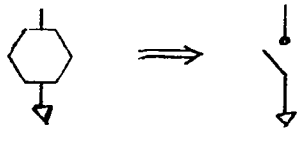
Electrical Simulation of Conventional Boundaries		

Figure 7. Plate Boundary Conditions — All Edges Simply-Supported

	Analytical	Analog
Deflection	$w(x, 0) = 0$ $w(x, \ell) = 0$ $w(0, y) = 0$ $w(\ell, y) = 0$	$\dot{w}$ Circuit 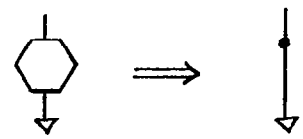
Slopes	$\theta_x(x, 0) = 0$ $\theta_x(x, \ell) = 0$	$\dot{\theta}_x$ Circuit 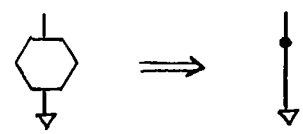
	$\theta_y(0, y) = 0$ $\theta_y(\ell, y) = 0$	$\dot{\theta}_y$ Circuit 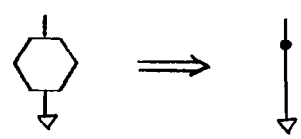
	$\theta_{xy}(0, y) = 0$ $\theta_{xy}(\ell, y) = 0$	$\dot{\theta}_y$ Circuit 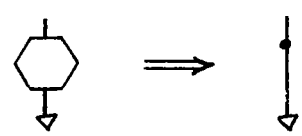
Electrical Simulation of Conventional Boundaries		

Figure 8. Plate Boundary Conditions — All Edges Clamped

slope circuits represent inductors to ground while the deflection circuit boundaries remain unchanged. The setting values of the boundary inductors in the slope circuits correspond to the magnitude of the bending flexibility of the elastic boundaries. For boundary conditions simulating a simply supported plate with viscous dampers distributed around the edges, the slope circuits appear as shown in Figure 7 while the deflection circuit boundaries are resistor-capacitor parallel combinations connected to ground. The setting values of the boundary resistors correspond to the reciprocal of the dashpot constants and the capacitors to the mass of the plate distributed along the edges.

By making use of symmetry conditions of the plate structure and external loading, the basic 5 x 5 grid circuit can be converted to simulate a quarter section of the plate. This procedure essentially increases the finite difference network from a 5 x 5 grid to a 9 x 9 grid. All computer data except that for the tapered plates are based on the 9 x 9 grid simulation.

To illustrate the scaling procedure, consider the computation of the basic setting values based upon the simply supported, uniform, square plate. For the 9 x 9 grid, Eq. (21) reduces to

$$\frac{P}{S} = \frac{\pi}{81} \frac{1}{f_{11}\,(\text{elec})} \frac{1}{\sqrt{L_1 C}} \tag{24}$$

where $\ell = 9\Delta x$. For electrical frequencies in the first mode of 100 cps and 150 cps, plots of the transformer ratio versus the $L_1 C$ product are shown as Figure 9. For a transformer ratio of unity and an electrical frequency of 100 cps, the $L_1 C$ product is

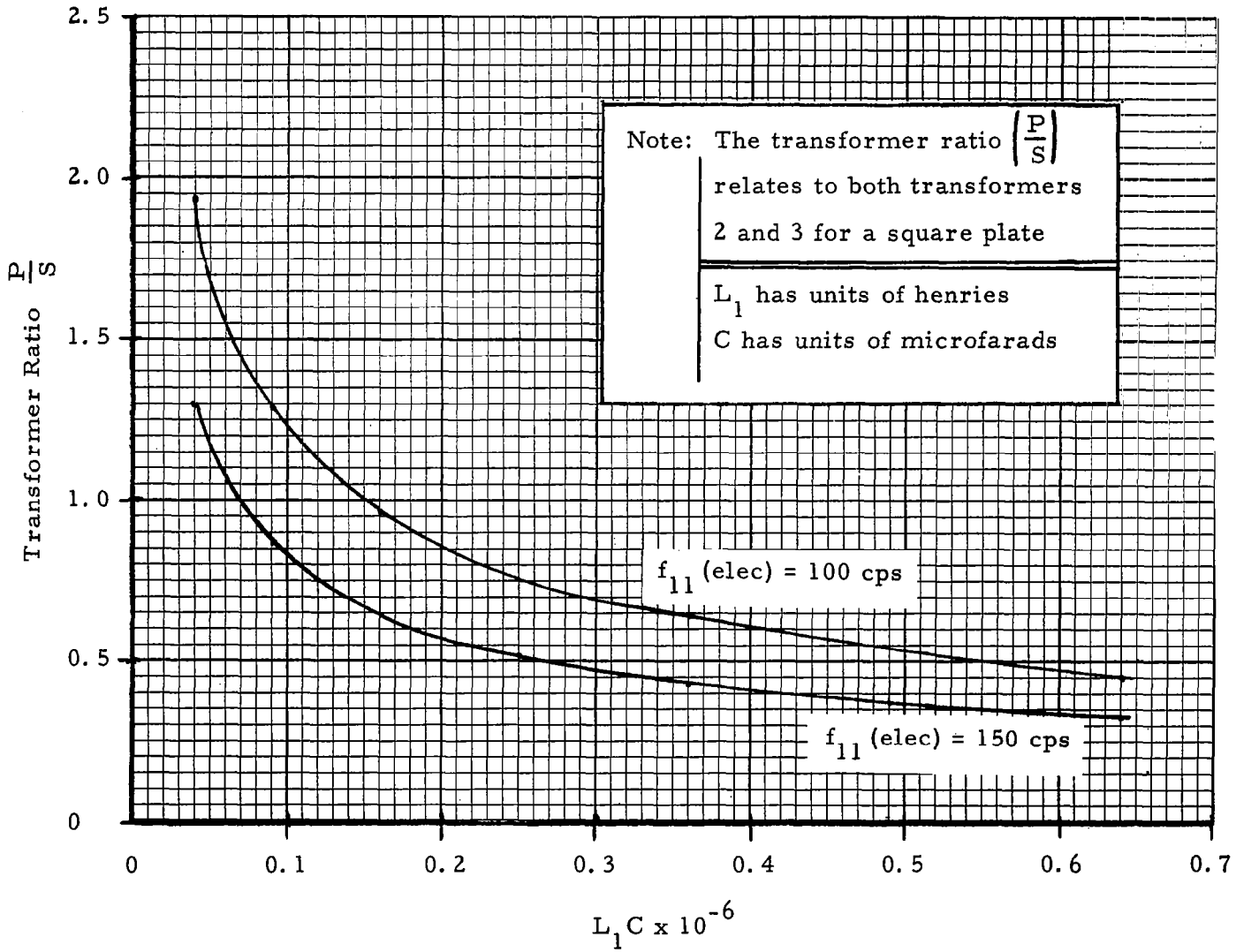

Figure 9. Transformer Ratio versus $L_1 C$ Product for Electrical Frequencies of 100 cps and 150 cps

$$L_1 C = 0.1510 \times 10^{-6} \tag{25}$$

Selecting $L_1 = 0.500$ h, the remaining component setting values become

$$C = 0.302\ \mu\text{fd}$$

$$L_2 = \frac{L_1}{1 - \nu^2} = 0.549 \text{ h}$$

$$L_3 = \frac{L_1}{2(1 - \nu)} = 0.355 \text{ h}$$

$$\frac{P}{S} = \frac{P_2}{S_2} = \frac{P_3}{S_3} = 1.00$$

$$\frac{P_1}{S_1} = \nu \frac{P}{S} = 0.300 \tag{26}$$

These setting values with the circuits of Figures 6 should yield a fundamental circuit resonance very close to 100 cps (electrical). This corresponds to a time scale factor of $N \simeq 1.205$.

3. COMPUTER RESULTS

3.1 FLEXIBLE BOUNDARY STUDIES

The effect of the flexible boundary on the fundamental modal frequency for the uniform and tapered plates is displayed by the curves of Figure 10. The ordinate is shown as a frequency ratio where the denominator f_{ss} denotes the fundamental modal frequency f_{11} of a simply supported, square, uniform plate. The abscissa represents a ratio of the plate flexural rigidity (D) to the stiffness of the flexible boundary (k_o) and extends theoretically from zero (fully clamped boundary conditions) to infinity (simply supported boundary conditions). The D/k_o ratio shown ranges from 0.1 to slightly above 10 and is noted to represent the region of maximum change in the frequency ratio. The ratios for the fully clamped boundaries are specified by the numerical values above the arrows along the y-axis whereas the ratios for the simply supported boundaries are specified by the numerical values for the vertically aligned arrows on the right-hand side of the curves.

For example, consider the fundamental frequency of a uniform square plate clamped along all of the edges to a flexible boundary. Assume the boundary to have a bending flexibility equal to the flexural rigidity of the plate. From the curve for the uniform plate in Figure 10 at $D/k_o = 1.00$, the desired frequency is found to be $f'_{11} \simeq 1.39\, f_{ss}$. The f_{ss} frequency must then be numerically evaluated according to Eq. (17) where $m = n = 1$. In a similar manner, f'_{11} modal frequencies for other flexible boundaries can be determined for uniform square plates as well as square plates with taper ratios of 1.33 and 2.00.

The fundamental mode shape of a uniform square plate for four values of boundary bending flexibilities is shown as Figure 11. Each of the four figures represents a quarter section of plate where ℄ denotes the lines of

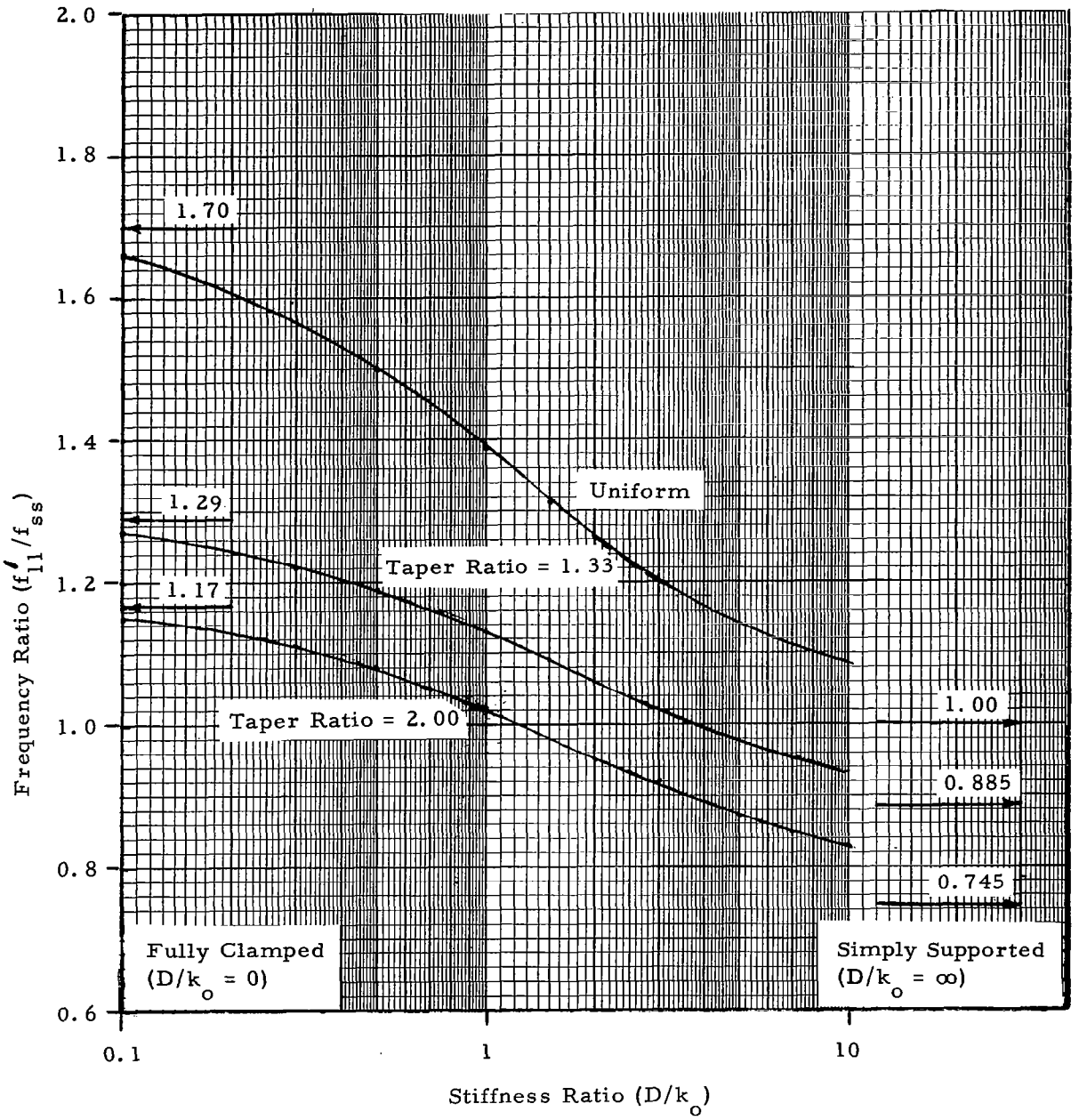

Figure 10. Effect of Boundary Stiffness on the Fundamental Modal Frequency of a Square Plate

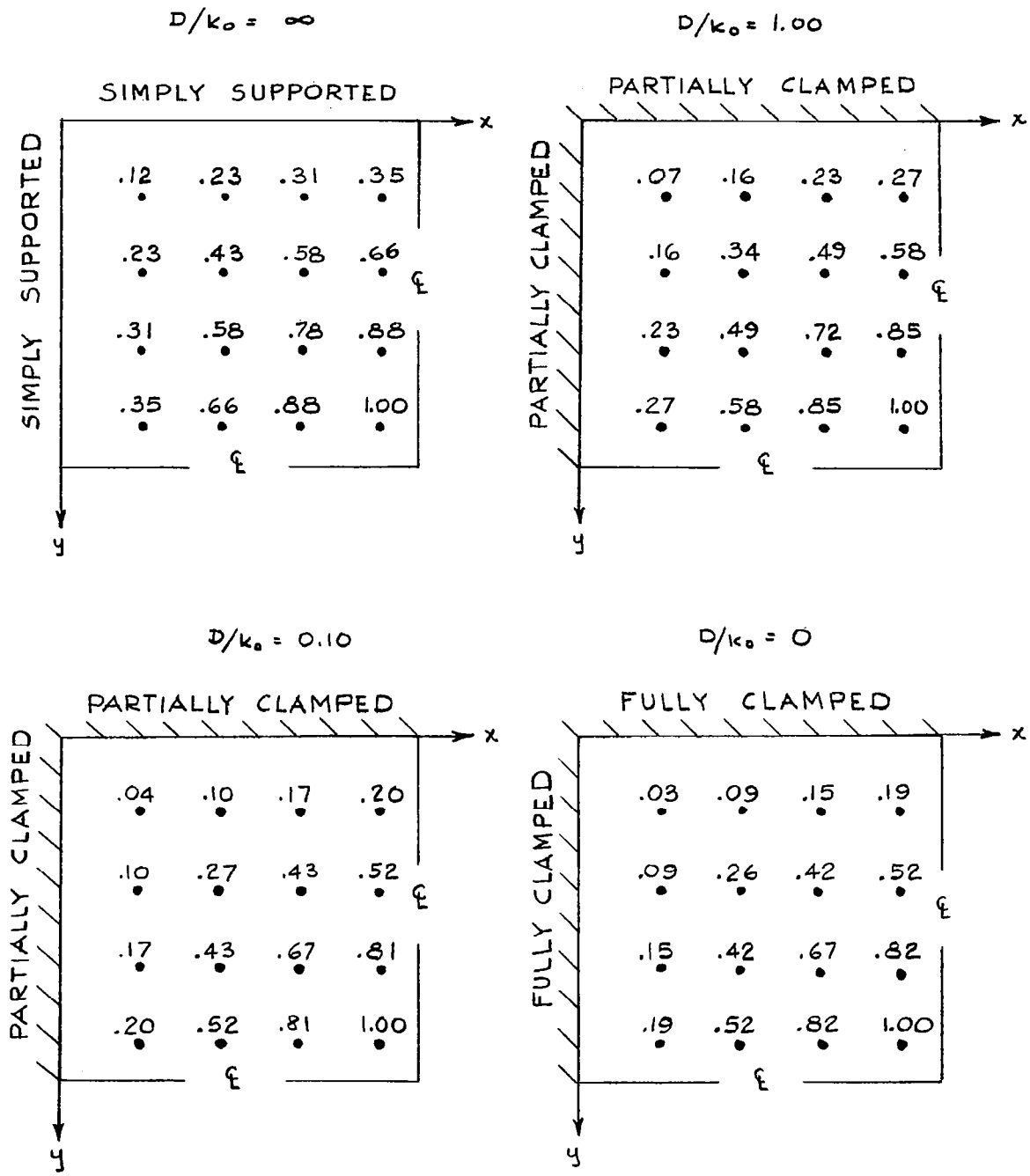

Note: Above values are at $\ell/9$ spatial positions.
A 9 x 9 finite difference grid is used for the plate simulation.

Figure 11. Effect of the Flexible Boundary on the Fundamental Mode Shape of a Flat, Square Plate

symmetry in the x and y dimensions. The mode shape values are located at $\ell/9$ spatial positions. The flexibility of the boundaries is changed uniformly at all of the edges and mode shapes are shown only for simply supported conditions ($D/k_o = \infty$), fully or rigidly clamped conditions ($D/k_o = 0$), and two intermediate boundary flexibilities of $D/k_o = 0.10$ and $D/k_o = 1.00$. Consistent with theory, the relative magnitudes at each spatial location become less as the boundary bending stiffness is increased and reache a minimum for the fully clamped conditions.

Figure 12 displays the fundamental mode shape for two tapered, square plates with four values of boundary bending flexibilities. Each of the figures represents a half section of plate and the modal values are shown at the $\ell/5$ spatial positions. The flexibilities are represented as D/k_o ratios and are noted as the same values which appear in Figure 11; $D/k_o = \infty$, 1.00, 0.10 and 0. The mode shape for the simply supported uniform plate is shown for reference. For each taper ratio, the relative magnitude of the mode shapes at each spatial location becomes less with increasing boundary restraint. Similar to the modal behavior for the uniform plate, the lowest values are observed at the fully clamped restraint.

While exploring for the $f_{1,3}$ modal frequency using the quarter plate simulation with fully clamped boundaries, two very closely spaced modal frequencies of 550 cps (electrical) and 542 cps (electrical) were observed. Similar behavior was noted for this mode with flexible bending restraints. For simply supported boundaries, however, this dual mode behavior disappeared and a single f_{13} modal frequency of 451 cps (electrical) was obtained. Such dual modal characteristics are consistent with theory (Reference 11) and are to be expected for square plates with uniformly clamped boundaries at all edges when the modal numbers are unequal but both even or both odd.

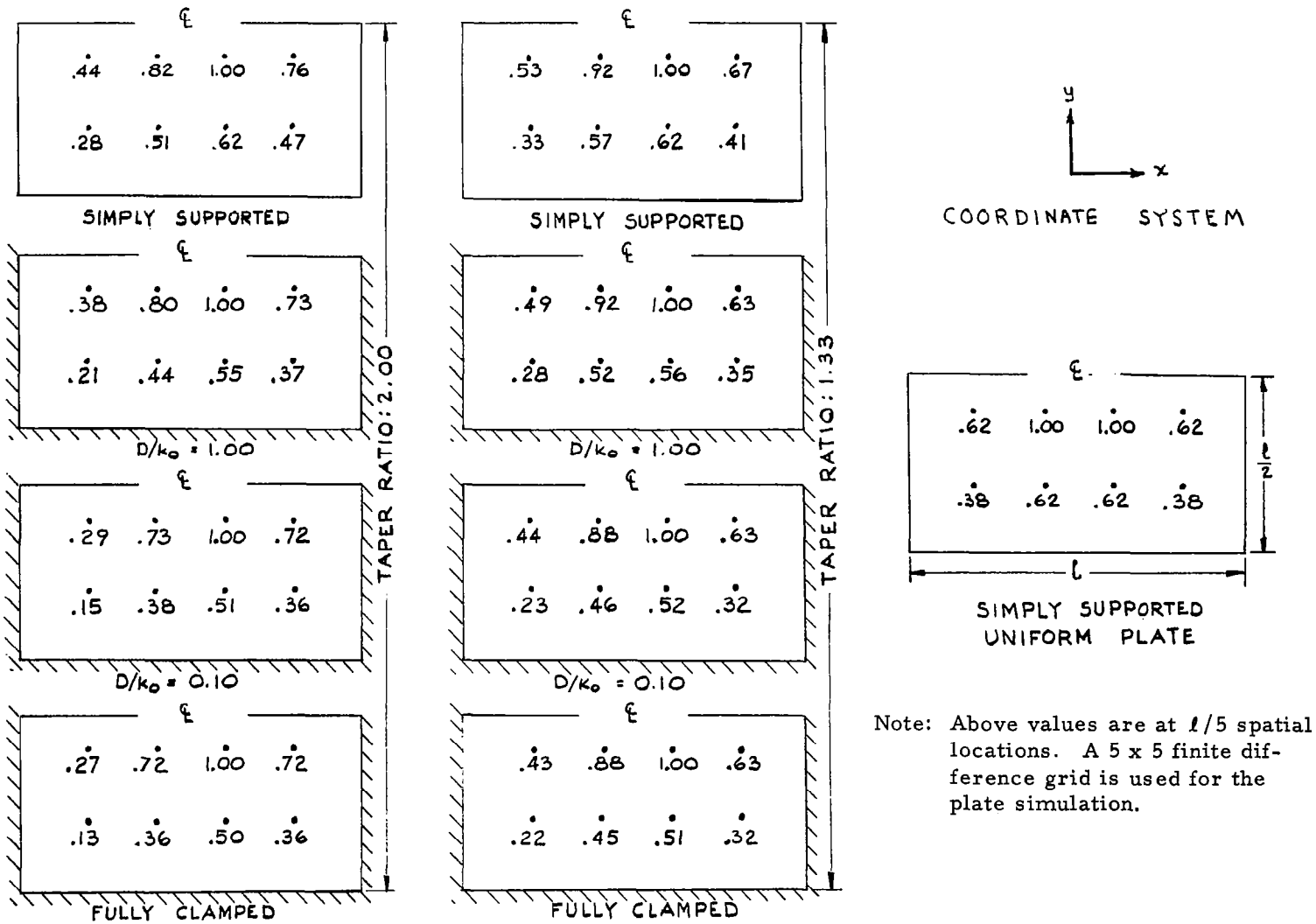

Note: Above values are at $\ell/5$ spatial locations. A 5 x 5 finite difference grid is used for the plate simulation.

Figure 12. Effect of the Flexible Boundary on the Fundamental Mode Shape of Tapered Square Plates

3.2 DAMPER EFFECTS STUDY

The dashpot effects are evaluated by considering the magnitude of the response at a point for both a limited area loading and a loading distributed over the entire surface of the plate. Depicted in terms of a full plate, the limited area loading and edge conditions are shown as Figure 13.

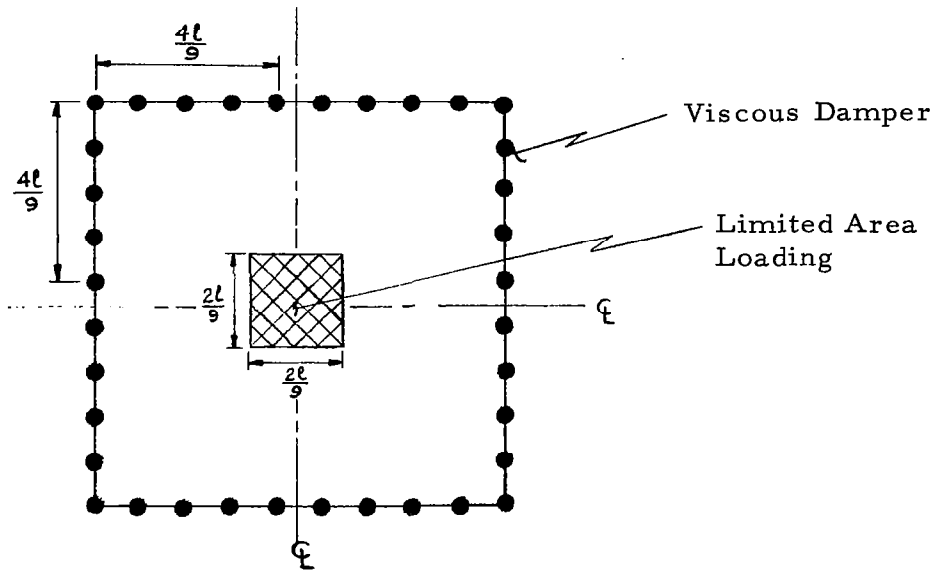

Figure 13. Area Loading on a Square Uniform Plate for Damper Effect Studies

All dashpots are varied uniformly and are set at different values for each test run. Since the applied loading and conditions of the plate structure are symmetric, only symmetric modes are excited.

Figures 14 and 15 are frequency response plots for the limited area loading. These four plots show the effect of four distinct dashpot setting values expressed as c/m ratios of zero, 3.08×10^4, 1.54×10^4, and 0.461×10^4. The zero c/m ratio corresponds to conventional simply supported boundary conditions. The response plots are based on a quarter

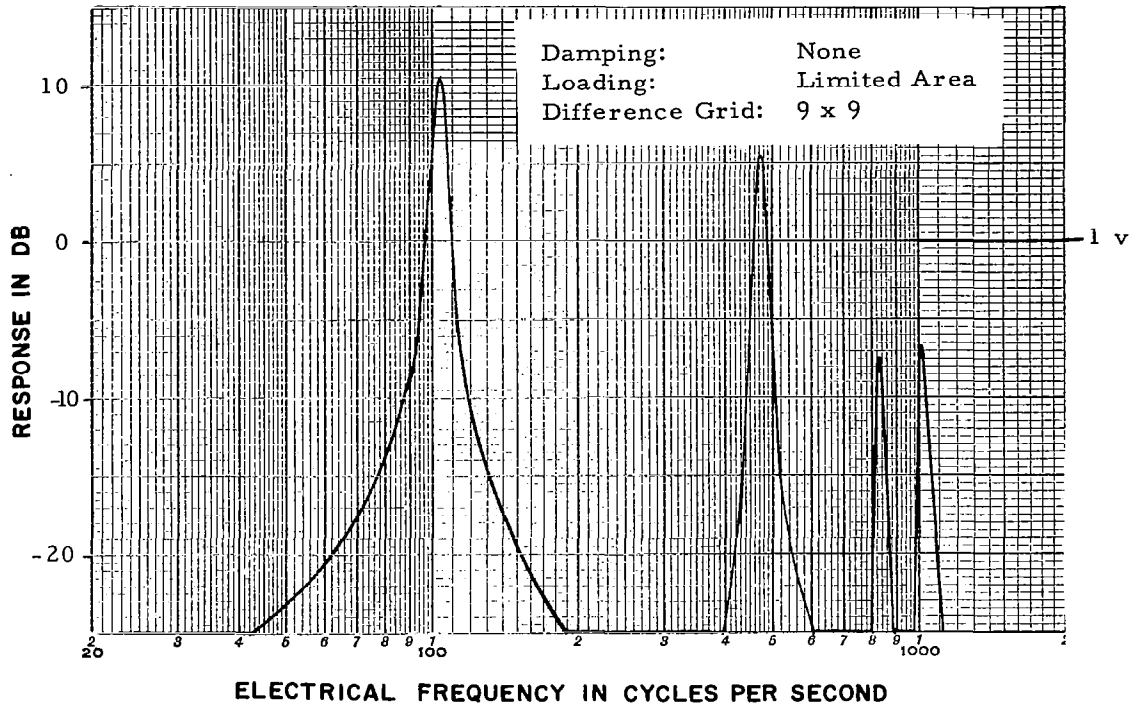

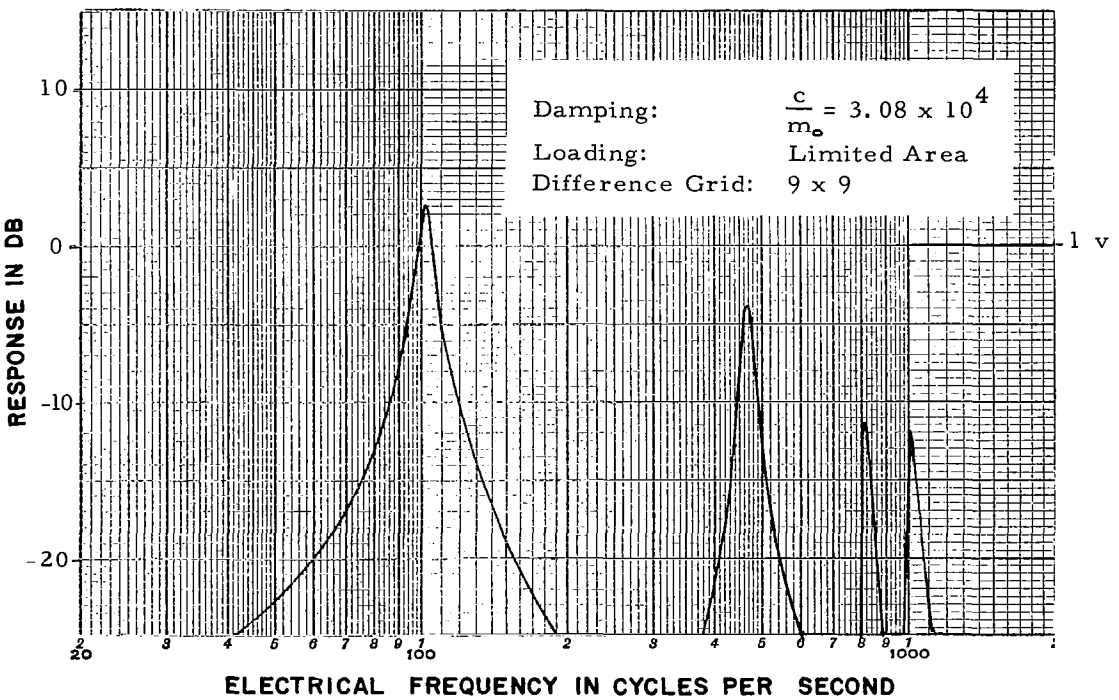

Figure 14. Effect of Edge Dampers on the Response Characteristics of a Simply Supported Square Plate

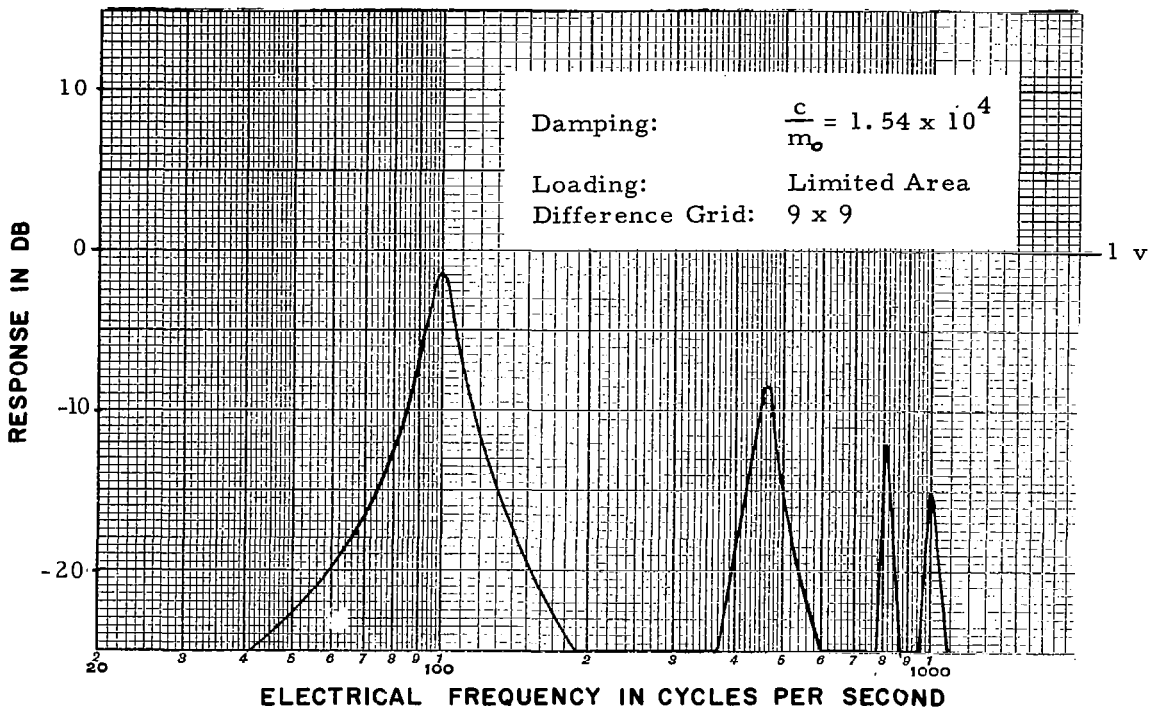

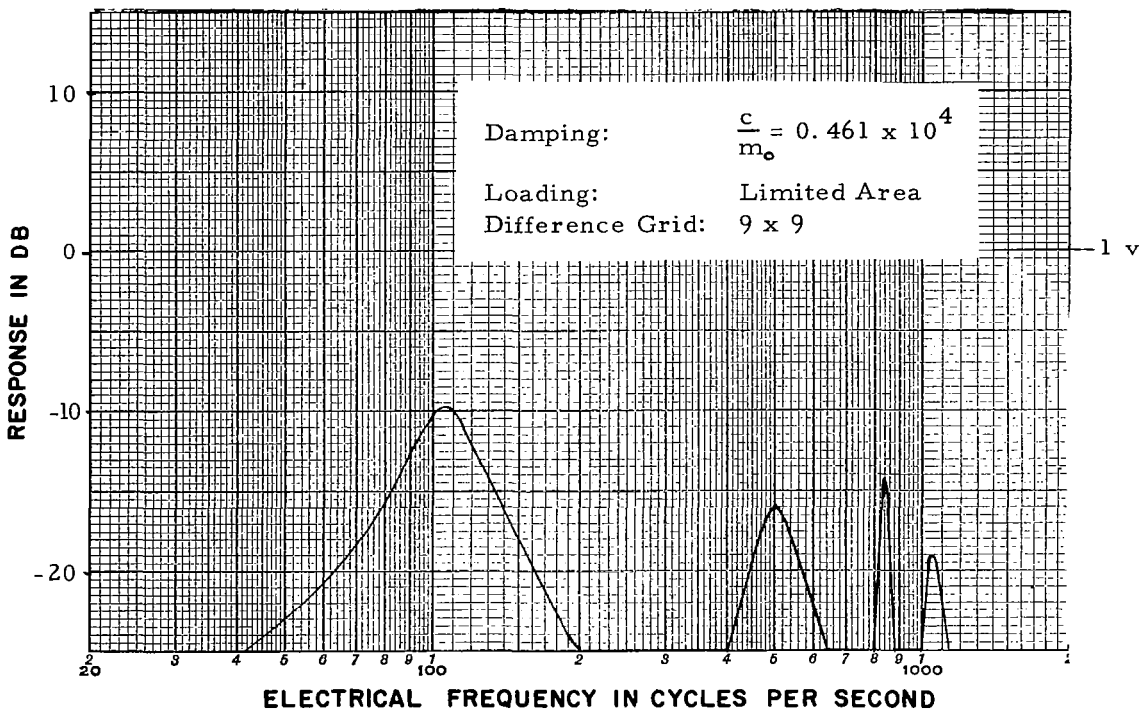

Figure 15. Effect of Edge Dampers on the Response Characteristics of a Simply Supported Square Plate

plate simulation and display the magnitude of the velocity (volts) at location $4\ell/9$, $4\ell/9$ due to an applied loading of 0.1 milliamps per quarter section. The response is shown as decibels (db) with 0 db corresponding to one volt while the frequency axis is the electrical frequency in cycles per second (cps). To convert the response values to the units of velocity (inches per second) per unit total load (pounds) $\left|\frac{\dot{w}}{F}\right|$ the voltages must be multiplied by 125. To convert electrical frequency to mechanical frequency, the electrical values are to be divided by the scale factor N, which equals ~ 1.205 for the 9 x 9 grid.

Figures 16 and 17 are response plots with test conditions identical to those of Figures 14 and 15 except the loading is uniformly distributed over the entire surface of the plate. Based on the quarter plate simulation, the response has units of volts and the applied loading was 0.02 milliamps per grid point (sixteen such points in the analog circuit). To convert the electrical response to units of velocity (inches per second) per unit total load (pounds), the voltages must be multiplied by 39.1.

With decreasing values of dashpot settings, the response in all modes decays in magnitude and the Q values for each of the modes tend to decrease. As used here, Q is indicative of the sharpness of the modal peaks and is defined as

$$Q = \frac{f_{mn}}{\Delta f_{mn}(\pm 3 \text{ db})} \tag{27}$$

where f_{mn} are the modal frequencies and $\Delta f_{mn}(\pm 3 \text{ db})$ is the half-power bandwidth of the mn mode. For small values of structural damping, this definition is consistent with the customary description of Q as the ratio of the center frequency to the half-power bandwidth.

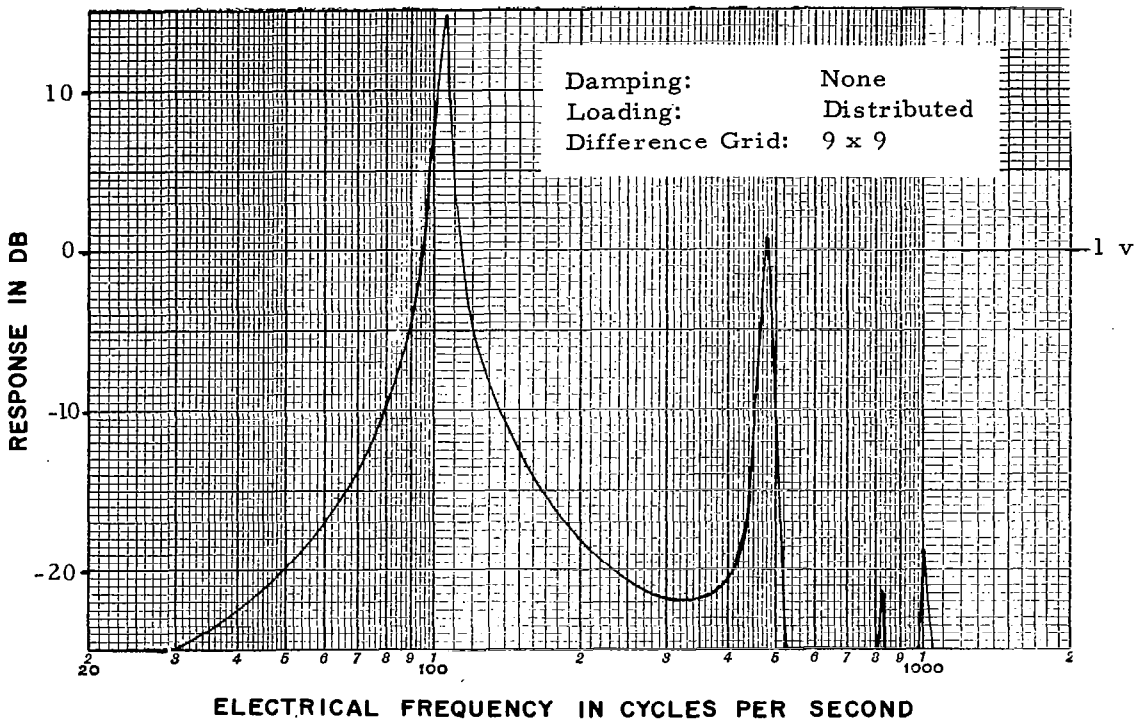

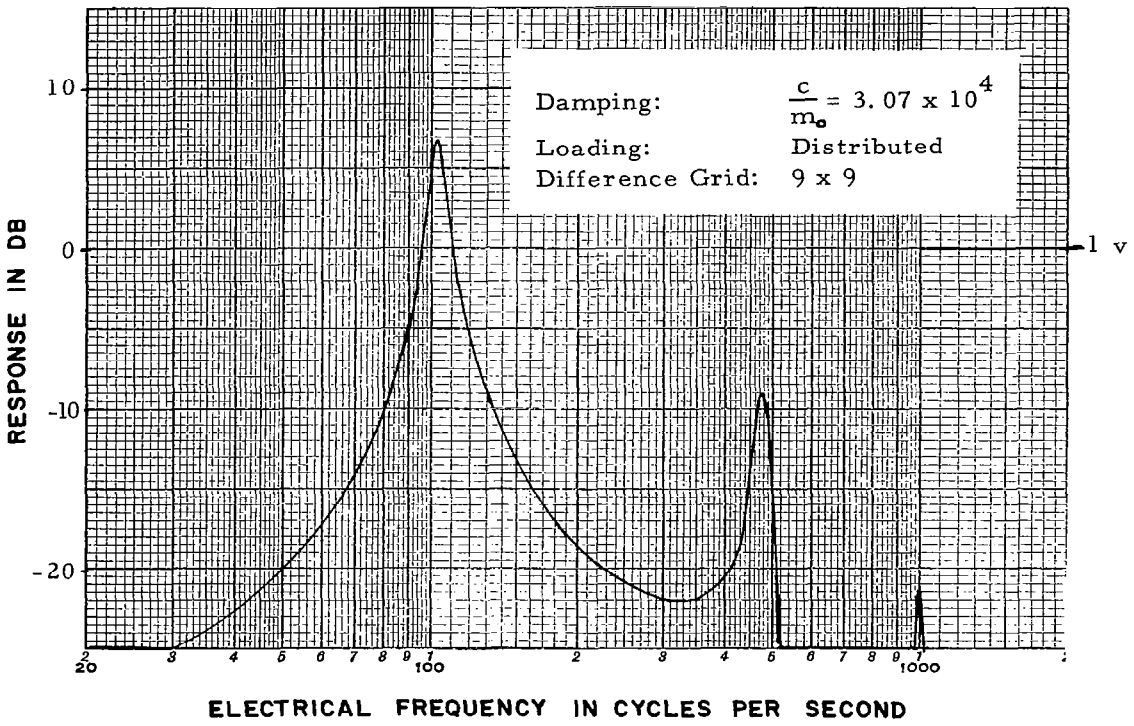

Figure 16. Effect of Edge Dampers on the Response Characteristics of a Simply Supported Square Plate

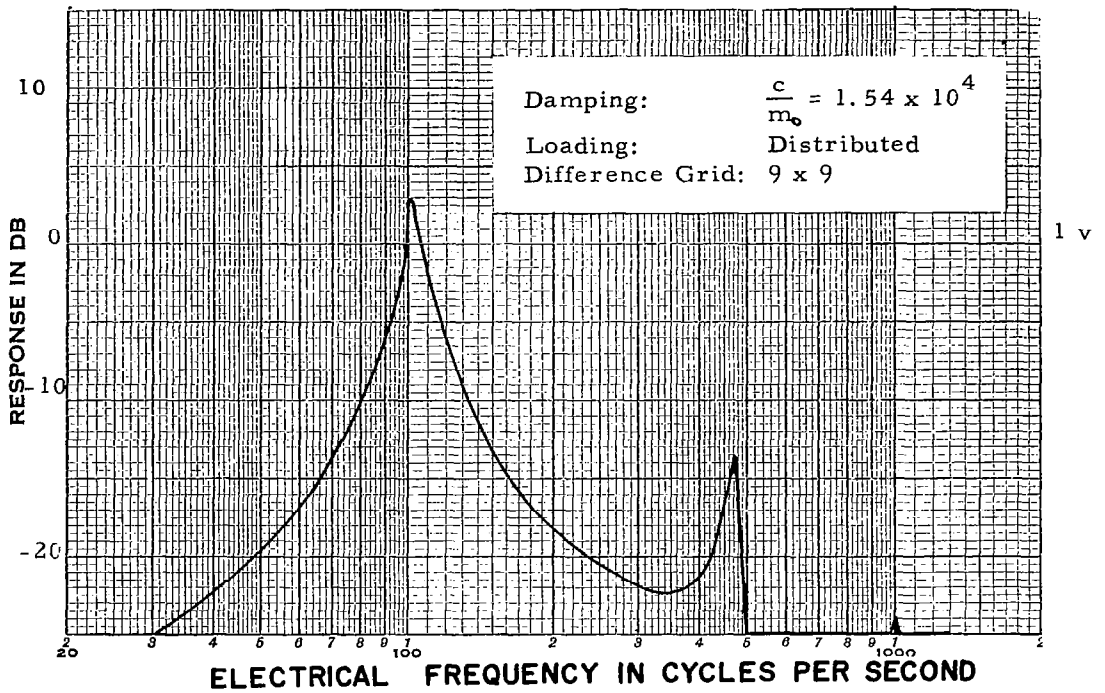

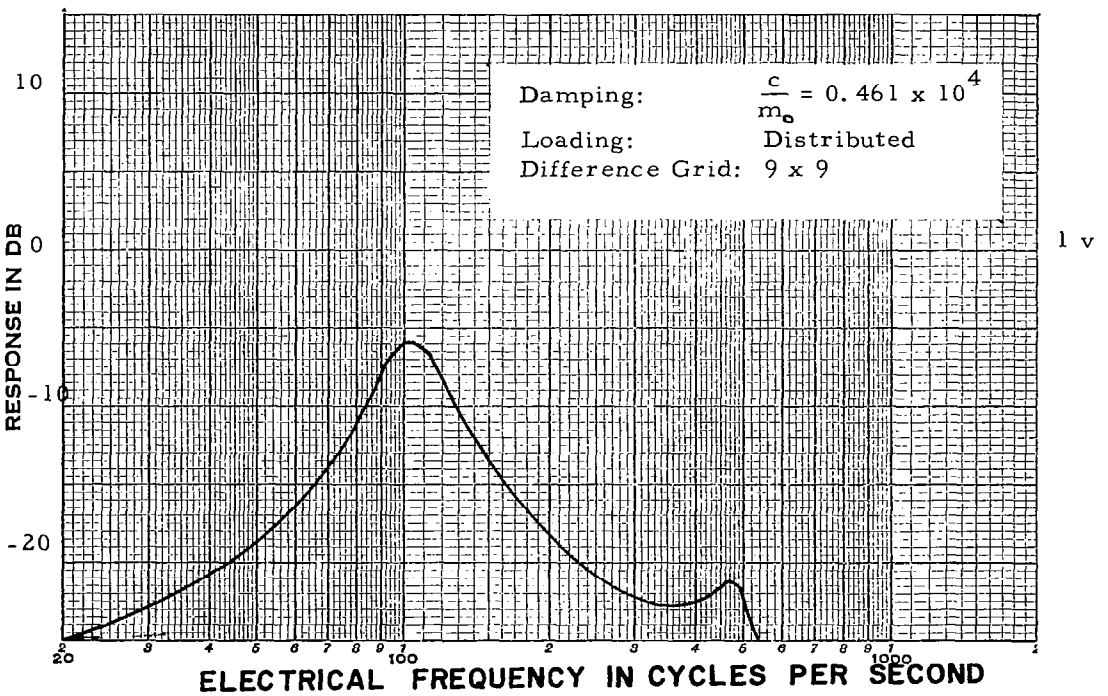

Figure 17. Effect of Edge Dampers on the Response Characteristics of a Simply Supported Square Plate

In general, the response in the higher modes is less than the response in the lower modes. Compared with the response maximum in the fundamental mode for simply supported boundaries, other f_{11} response maxima for various values of edge dampers are shown in Figure 18. Expressed as a percentage reduction of the response for simply supported edges, the data of Figure 18 appears as Figure 19. In both plots, the abscissa theoretically extends from the simply supported conditions ($c/m_o = \infty$) to a fully suspended condition ($c/m_o = 0$) where the total energy of the applied loading is dissipated. The range of the shown c/m_o values includes the maximum effect of the dampers on the response to harmonic motion.

3.3 ERRORS

The most significant errors inherent in the passive circuits are associated with the finite-difference representation of the distributed structure. For a uniform square plate with simply supported boundary conditions at all edges, the ratio of modal frequencies for finite difference and distributed models is

$$\frac{\omega'_{mn}}{\omega_{mn}} = \frac{4 N_0^2}{\pi^2 (m^2 + n^2)} \left[\sin^2\left(\frac{m\pi}{2 N_0}\right) + \sin^2\left(\frac{n\pi}{2 N_0}\right) \right] \tag{28}$$

In this equation, ω'_{mn} is the mn modal frequency for a finite difference model, ω_{mn} is the mn modal frequency obtained by solving the partial differential equation for a plate and given as

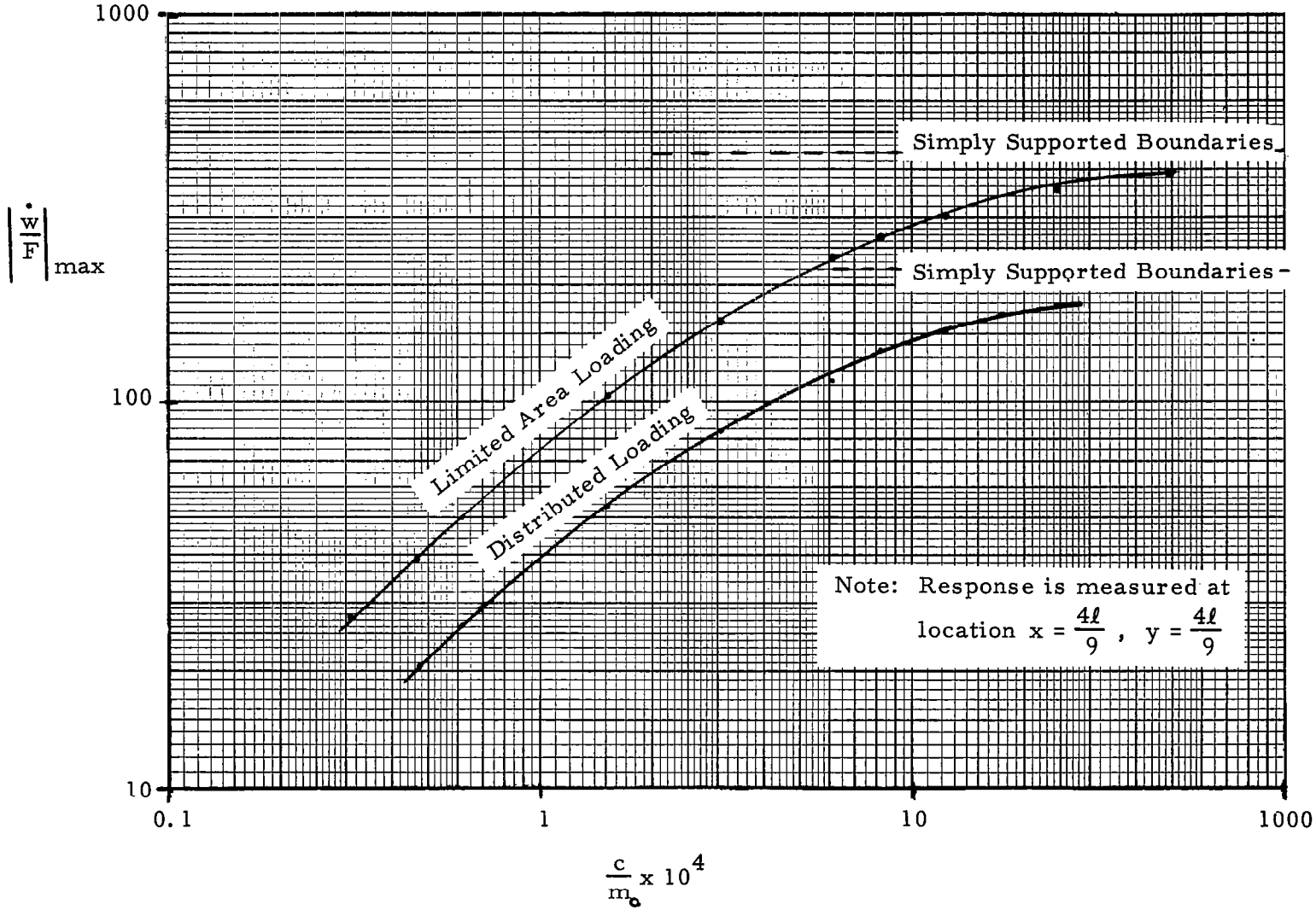

Figure 18. Typical Effect of Edge Dampers on the Magnitude of the Maximum Response per Unit Total Load for a Uniform Square Plate

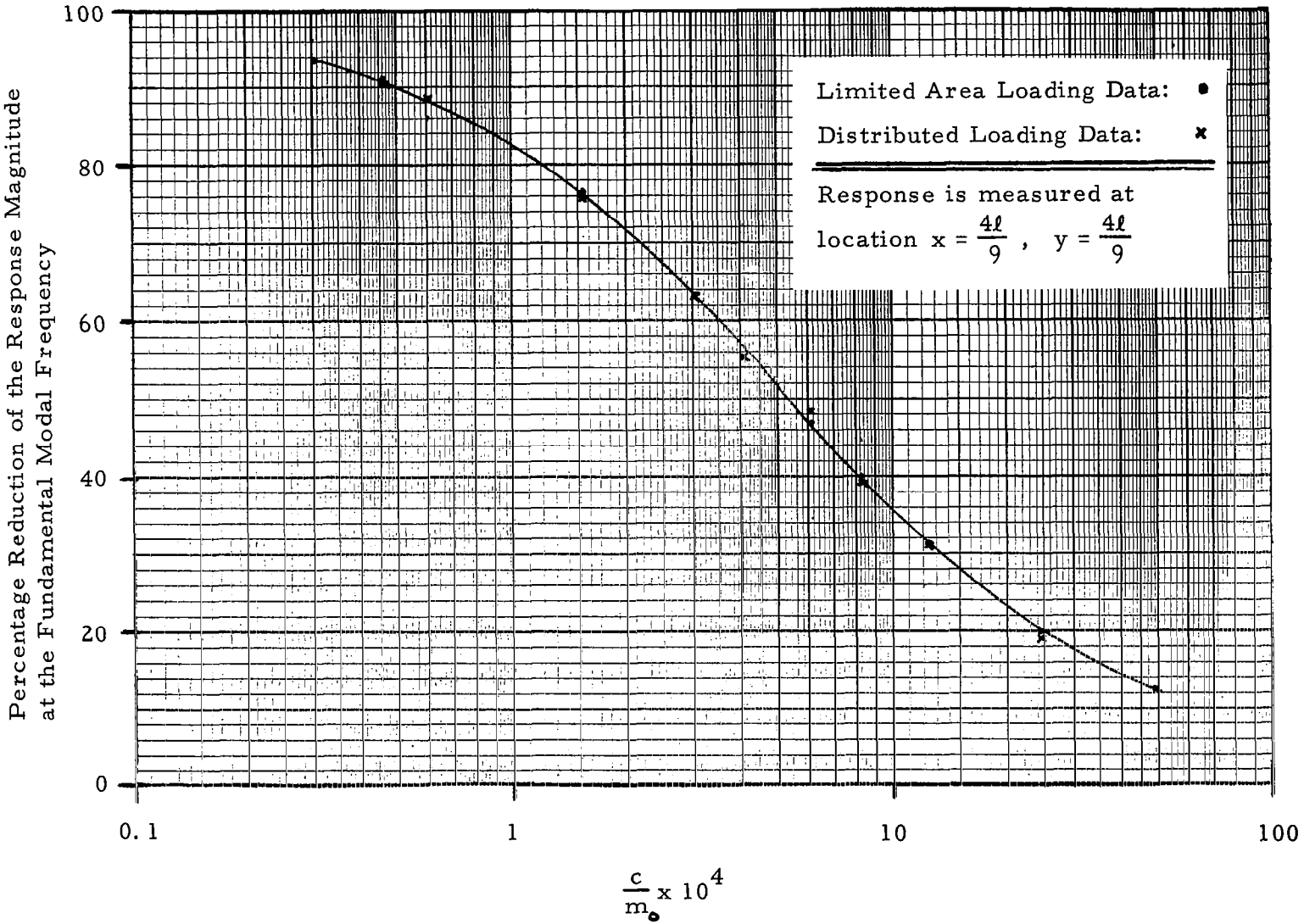

Figure 19. Percentage Reduction of the Maximum Response Due to Viscous Edge Dampers

$$\omega_{mn} = \left(\frac{\pi}{\ell}\right)^2 (m^2 + n^2)\sqrt{\frac{D}{m_o}} \tag{29}$$

where m and n are the number of half waves in the x and y directions, and N_0 the number of finite difference grids. Plotted as a percentage of ω_{mn}, the modal frequency errors due to finite difference approximations for various grid sizes are shown as Figure 20. As the grid size is increased, the error in all modes is reduced with the least error associated with the fundamental mode. These curves strikingly depict the reason for maximizing the difference grid per computer size for any problem.

The modal frequency errors associated with the grids used in the plate simulation of this study are tabulated as Figure 21. The results for the passive analog simulation are the values obtained on the analog computer and the percentages denote the variations from the analytical solution. The differences between the finite difference and passive analog errors represent errors due to computer parasitics. These parasitics errors are small compared to difference errors and are due to stray impedances resulting from imperfect circuit components and computer layouts.

The finite difference error is dependent also on the boundary conditions as is reflected in the ratio of the fundamental modal frequencies for fully clamped and simply supported boundary conditions. From the data for a uniform plate shown in Figure 10, the frequency ratio obtained from analog computer data is 1.70 as contrasted with 1.83 obtained from theoretical expressions developed by Warburton in Reference 11. This represents a discrepancy of 7.1% and represents an approximate upper bound for difference error in the fundamental mode of a uniform plate simulated with a 9 x 9 grid.

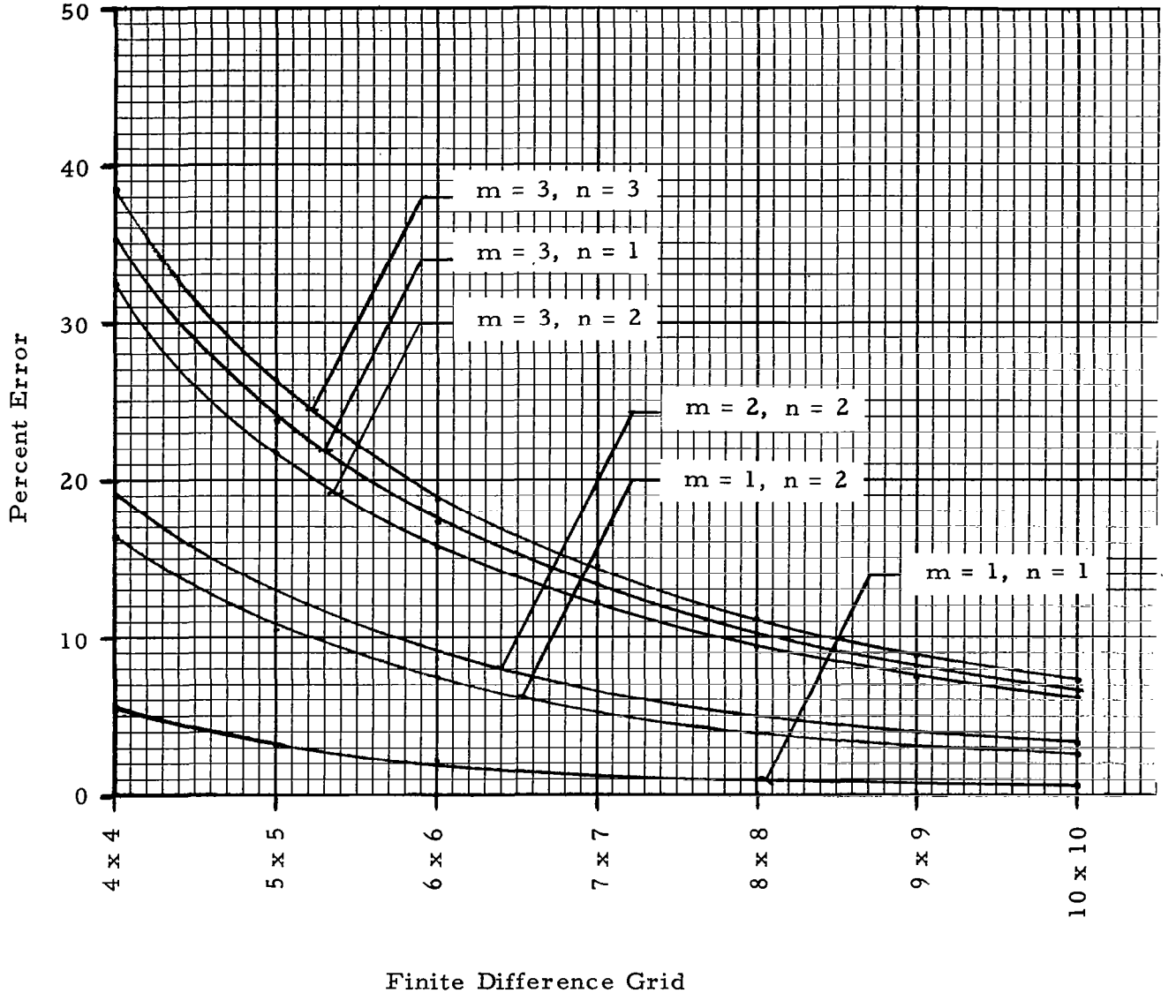

Figure 20. Finite Difference Error for a Square Plate Simply Supported at all Edges

Procedure			Modal Frequencies (cps)			
			f_{11}	f_{12}	$f_{1,3}$	f_{33}
	Analytical	Solution to Differential Equation	83	208	415	748
	Passive Analog Simulation	5 x 5 Grid	80.3	182	322	
			3.26%	12.48%	22.4%	
		9 x 9 Grid (1/4 Plate)	83		375	658
			0%		9.6%	12.0%
	Finite-Difference Error	5 x 5 Grid	3.1%	10.4%	23.8%	26.3%
		9 x 9 Grid (1/4 Plate)	1.01%	3.40%	8.03%	8.81%

Figure 21. Modal Data Comparisons for a Square Plate Simply Supported at all Edges

REFERENCES

1. Barnoski, R. L., "Electrical Analogies and the Vibration of Linear Mechanical Systems," NASA-CR 510, National Aeronautics and Space Administration, Washington, D. C., June 1966.

2. Barnoski, R. L., and C. R. Freberg, "Passive Element Analog Circuits for Three Dimensional Elasticity," Transactions of the ASME Journal of Engineering for Industry. August 1966.

3. Bush, V., "Structural Analysis by Electric Circuit Analogies," Journal of the Franklin Institute, Vol. 217, March 1934, p 289.

4. Firestone, F. A., "A New Analogy between Mechanical and Electrical Systems," Journal of the Acoustical Society of America, Vol. 4, 1933, pp 249-267.

5. Freberg, C. R., and E. N. Kemler, Elements of Mechanical Vibrations, John Wiley and Sons, Inc., New York, August 1960.

6. Higgins, T. J., "Electroanalogic Methods," Applied Mechanics Reviews, 1956-1958. Reprints available from Director, Engineering Experiment Station, M. E. Building, University of Wisconsin, Madison, Wisconsin.

7. Kirchhoff, G., "Flow of an Electric Current Through a Plane, Particularly Through a Circular Disk (in German)," Ann. Phys. und Chemie, 64, 1845, p 499.

8. MacNeal, R. H., Electric Circuit Analogies for Elastic Structures, John Wiley and Sons, Inc., New York. 1962.

9. Ryder, F. L., "Energy Versus Compatibility Analogs in Electrical Simulators of Structures," Journal of the Aero/Space Sciences, February 1959, pp 108-116.

10. Timoshenko, S., and S. Woinowsky-Krieger, Theory of Plates and Shells, McGraw-Hill Book Co., Inc., New York, 1959.

11. Warburton, G. B., "The Vibration of Rectangular Plates," 1953, Proceedings of the Institution of Mechanical Engineers (A), Vol. 167.

NASA-Langley, 1967 CR-666